

**Zeitschrift:** IABSE reports = Rapports AIPC = IVBH Berichte  
**Band:** 75 (1996)

**Rubrik:** Session 5: Modelling of connection behaviour 1

### **Nutzungsbedingungen**

Die ETH-Bibliothek ist die Anbieterin der digitalisierten Zeitschriften auf E-Periodica. Sie besitzt keine Urheberrechte an den Zeitschriften und ist nicht verantwortlich für deren Inhalte. Die Rechte liegen in der Regel bei den Herausgebern beziehungsweise den externen Rechteinhabern. Das Veröffentlichen von Bildern in Print- und Online-Publikationen sowie auf Social Media-Kanälen oder Webseiten ist nur mit vorheriger Genehmigung der Rechteinhaber erlaubt. [Mehr erfahren](#)

### **Conditions d'utilisation**

L'ETH Library est le fournisseur des revues numérisées. Elle ne détient aucun droit d'auteur sur les revues et n'est pas responsable de leur contenu. En règle générale, les droits sont détenus par les éditeurs ou les détenteurs de droits externes. La reproduction d'images dans des publications imprimées ou en ligne ainsi que sur des canaux de médias sociaux ou des sites web n'est autorisée qu'avec l'accord préalable des détenteurs des droits. [En savoir plus](#)

### **Terms of use**

The ETH Library is the provider of the digitised journals. It does not own any copyrights to the journals and is not responsible for their content. The rights usually lie with the publishers or the external rights holders. Publishing images in print and online publications, as well as on social media channels or websites, is only permitted with the prior consent of the rights holders. [Find out more](#)

**Download PDF:** 01.04.2026

**ETH-Bibliothek Zürich, E-Periodica, <https://www.e-periodica.ch>**



**SESSION 5**

**MODELLING OF CONNECTION BEHAVIOUR 1**

Leere Seite  
Blank page  
Page vide



## Modelling of semi-rigid connections : column bases.

**Jean-Pierre JASPART**  
Research Associate FNRS  
Doctor Engineer  
University of Liège

**Didier VANDEGANS**  
Civil Engineer  
CRIF Steel Construction Dpt.

Liège  
BELGIUM

Jean-Pierre Jaspert, born in 1962, got his Civil Engineering Degree in 1985 and his Ph.D Degree in 1991.

He is the author of more than 60 papers on connection and frame design, one of the member of the Drafting Group of EC3, Annex J and Chairman of the COST C1 Working Group on *Steel and Composite Connections*.

Didier Vandegans, born in 1971, got his Civil Engineering Degree in 1994 at the University of Liège. His main domain of activity is the semi-rigid connections.

### Summary

The column bases have a high semi-rigid behaviour. In this paper, a mechanical model to predict their moment-rotation response is presented. To achieve this goal, the component method described in Annex J of Eurocode 3 (EC 3) is used and extended. Comparisons with experimental tests is performed.

### 1. Introduction

In the daily practice, the column bases are usually considered as rigid or pinned. Experiments have shown, that in fact, they can have a high semi-rigid behaviour which influences the frame response; in particular the frame lateral deflections and the frame stability in unbraced frames, the columns stability in braced frames. Taking this semi-rigid effect into account leads to significant cost savings linked to the reduction of the man power necessary to realise rigid column bases (less stiffening) or of that of the column size in case of pinned column bases.

Analytical formulas are now available to evaluate the strength of the column bases. The prediction of the stiffness is much more complex, because of the influence of the normal force and of the loading history.

A way to solve the problem of loading history is to develop a mechanical model, based on the component method, which can react by itself to the applied forces. Such mechanical model is described in this paper and the comparisons with experimental tests are shown.



## 2. Test description

Twelve experimental tests have been carried out recently in Liège [3]. The general configuration is the same for each of them and is described on figure 1

The column profiles are HEB 160 made of S355 steel.

Two sorts of configurations are considered :

- connections with two anchor bolts (traditionally considered as pinned);
- connections with four anchor bolts (traditionally considered as rigid)

Two different thicknesses for end-plate are used : 15 and 30 mm.

A normal compression force is first applied to the column; it remains constant during the whole test. In a second step, the bending moment is progressively increased.

Three different values of normal force are applied : 100 kN, 600 kN and 1000 kN.

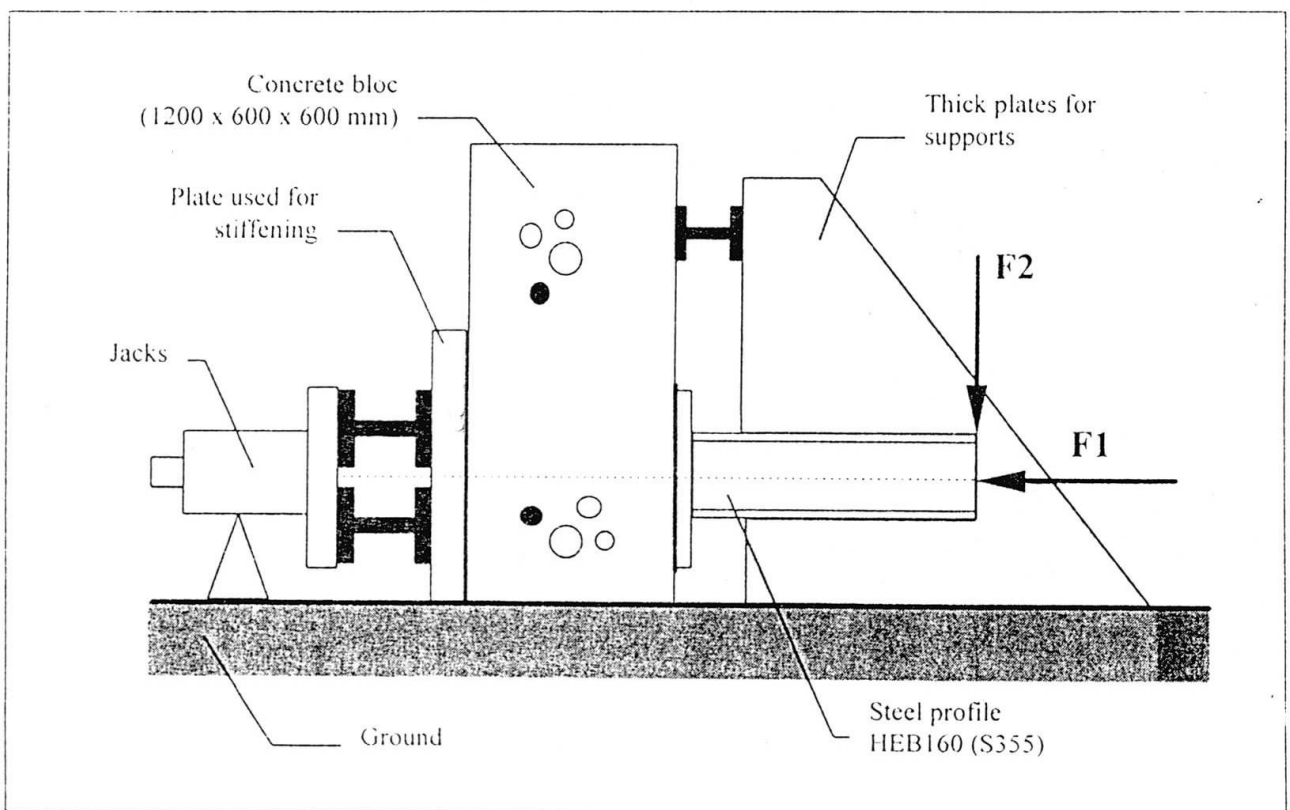


Fig. 1. Test configuration.

### 3. Experimental curves

Because of the connection deformability and of the high applied normal forces, second order effects cannot be neglected when interpreting the test results. Figure 2 shows how the bending moment in the connection is influenced by the compressive force in the column.

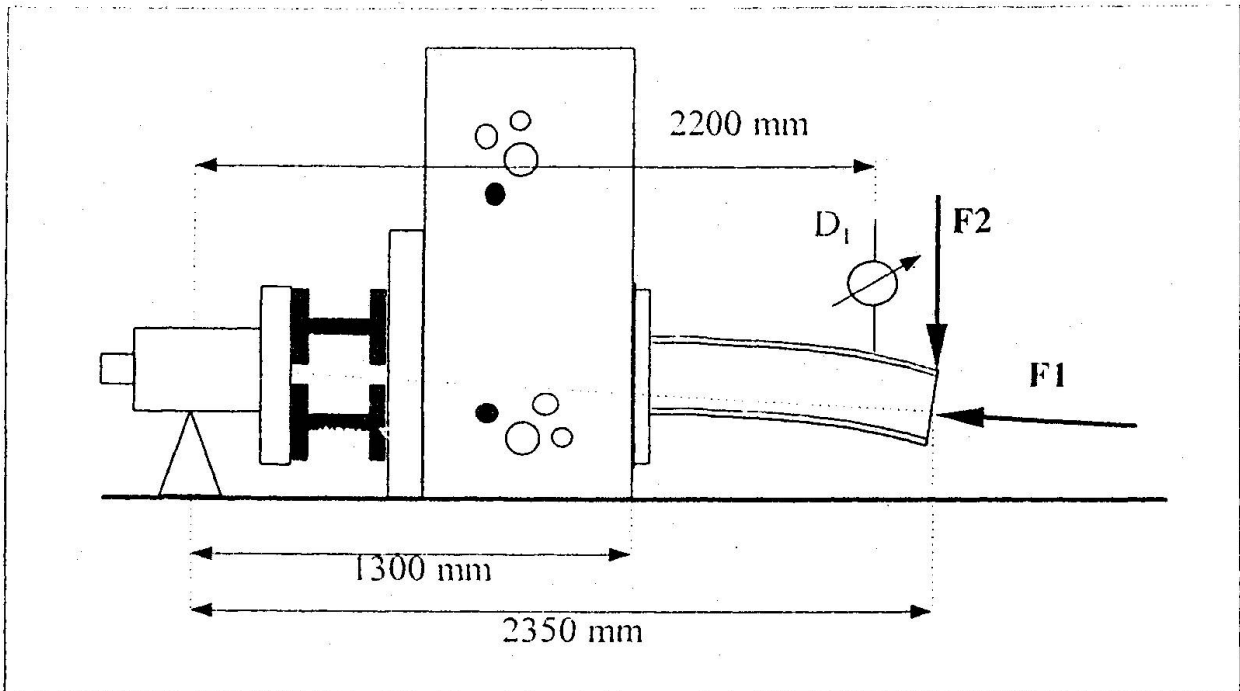


Fig. 2. Determination of the joint bending moment.

Figure 3 shows a comparison between the moment-rotation curves for the tests with 2 and 4 anchor bolts in the case of a 15 mm thick end-plate.

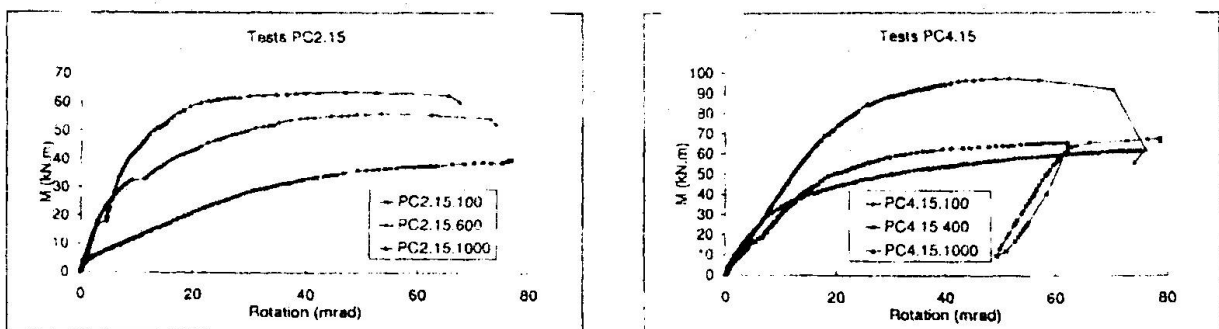


Fig. 3. Moment rotation curves

While examining these figures, it can be seen that the highest the normal force in the column, the highest the bending resistance of the joint. For tests with similar geometries, the initial stiffness seems not to be affected by the value of the normal force in the column. For higher



moments, the stiffness of the connection decreases when there is a loose of contact between the plate and the concrete in the tension zone. This loose of contact appears earlier for a low normal force in the column.

## 4. Mechanical modelling

### 4.1 Generals

The aim is to develop a model for column bases, based on the component method described in Annex J of Eurocode 3 [1]. First it is necessary to identify the different behaviour aspects to be covered in order to describe correctly the behaviour of the column bases.

According the observations made during the experimental tests, it can be said that :

- the contact between the plate and the concrete is a complex phenomenon, which must be modelled in a very refined way;
  - the bond between the anchor bolts and the concrete is quickly broken. Therefore, it might be assumed that the anchor bolts are free to extend in tension, from the beginning of the loading;
  - under the column flange in compression, the plate deforms significantly. Therefore, the pressure under the plate is far from being uniform, even under central compression. The concept of the equivalent rigid plate to which it is referred to in EC 3 Annex L [2] is kept in this model;
  - in the compression zone, the extended part of the plate has a very high influence, because it prevents crushing in the concrete. The development of a plastic line is observed in the extended part during the test. This plastic line requires a large deformation energy and it is necessary to model it;
  - a plastic hinge may form in the steel profile. This can lead to significant local deformations. In order to compare the mechanical model to the experimental moment-rotation curves (which include these deformations), it is imperative to take this source of deformation into account;
  - the column base deforms during the loading. In particular the contact zone and the lever arm of the internal forces are changing.
- Furthermore, the behaviour of each component (concrete, anchor bolts, plate, profile, ...) is non linear. Therefore, only an iterative procedure allows to describe correctly the connection behaviour for the whole loading.

The mechanical model shown in figure 4 is based on these observations.

The following components can be identified :

- 1) extensional springs for the deformation of the profile. They are working in tension and compression;
- 2) extensional springs for the deformation of the anchor bolts and the plate subjected to transverse anchor bolt force. Only one spring is used for an anchor bolt row. It works only in tension;
- 3) extensional springs for the concrete under the plate; they work only in compression;

- 4) springs in bending for the plastic deformation of the plate in the compression zone(s).  
These springs are activated when the extended part of the plate in the compression zone is subjected to contact forces with concrete.

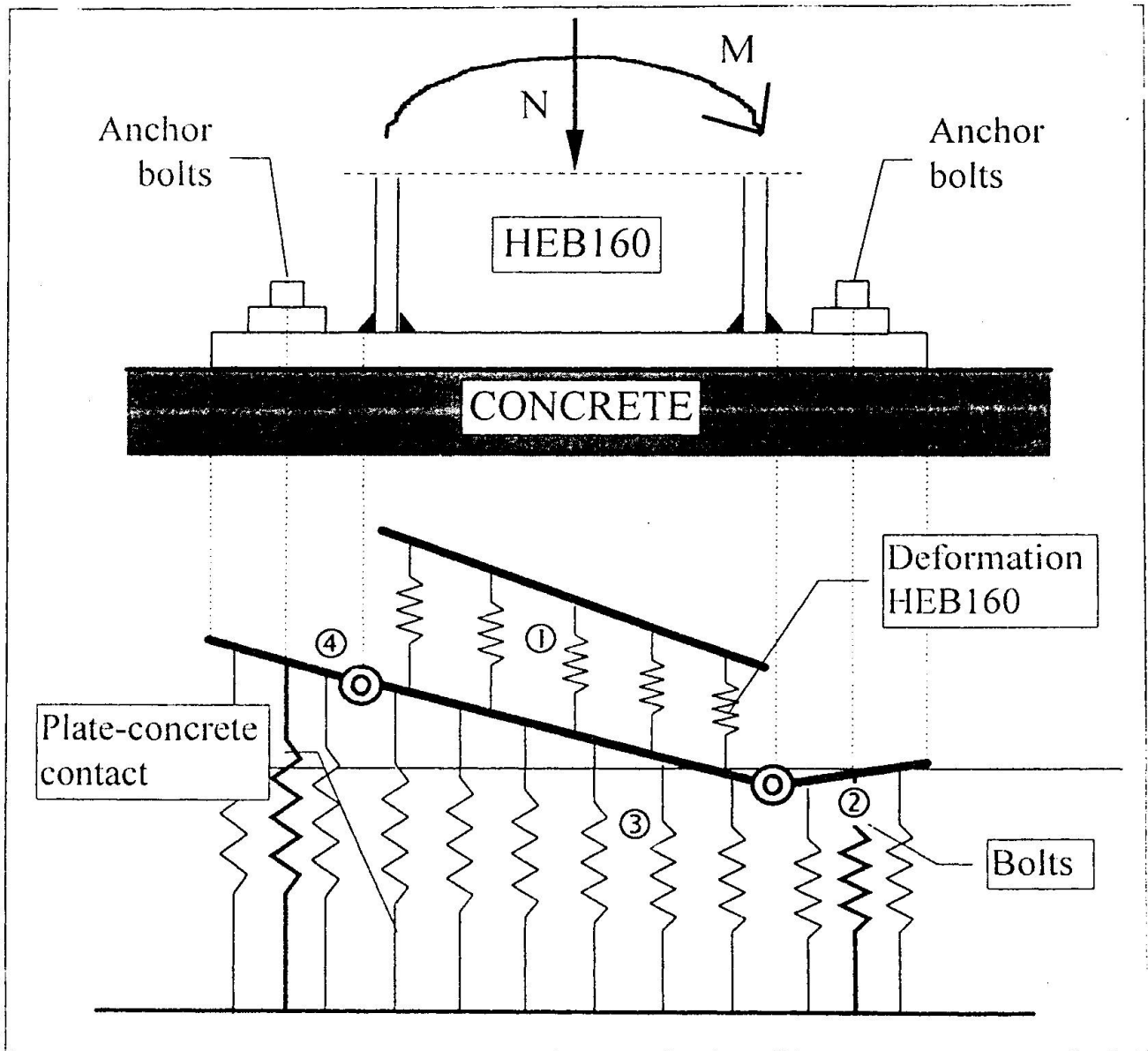


Fig. 4. Modelisation of the column bases connections

## 4.2 Behaviour of the individual components

### 4.2.1 Concrete

The plate-concrete contact is a very complex phenomenon, because the contact zone varies with the eccentricity of the compressive forces as well as with the flexibility of the plate, directly linked to its thickness.



The concept of equivalent rigid plate described in Annex L of Eurocode 3 is kept. Figure 5 shows how the plate is idealized. It might be surprising to keep a so large equivalent plate outside the flange, but this part has not a very high influence on the connection behaviour.

The behaviour law  $\sigma - \varepsilon$  adopted in the model is the classical parabolic-rectangular law. The concrete-plate contact is modelled by a finite number of springs: each of them corresponds to a small part of the contact zone. A hundred of such springs leads to a good level of accuracy.

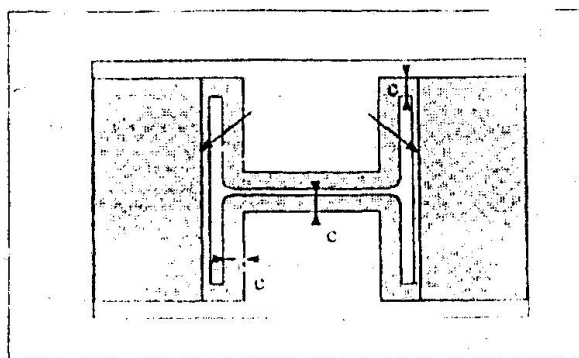


Fig. 5. Equivalent rigid plate

#### 4.2.2 Anchor bolts and plate

The local response of the anchor bolts in tension and the plate depends on the thickness of the plate and of the position of the bolt rows : inside or outside the flange.

EC 3 Annex J is used for the determination of the behaviour curve of these components. For the end-plate deformability, it has been assumed that no prying effect occurs between the concrete and the edge of the end-plate in the tension zone. This assumption is justified as follows :

- the anchor bolts have a very high deformability. Therefore the resulting relative displacement between the plate and the concrete is significant; sufficiently to be considered as higher than that due to the flexural deformation of the plate, excepted for very thin plates, but these ones are usually not used for column bases;
- the prying effects result from a concrete-to-plate contact. Even if this contact develops, the high deformability of the concrete under these concentrated forces prevents an important prying force to develop as in case of steel-to-steel contact.

In the compression part, the plate also deforms. Tests have shown that this deformation is very local and can be assimilated to a plastic hinge. This one is modelled through the use of a spring in bending characterized by an elastic-plastic law in the compression zone. The spring is infinitely rigid in the tension zone.

#### 4.2.3 The steel profile

Because of the high normal forces in the column, this one might partially yield. An elastic-plastic behaviour law is adopted for the related springs.

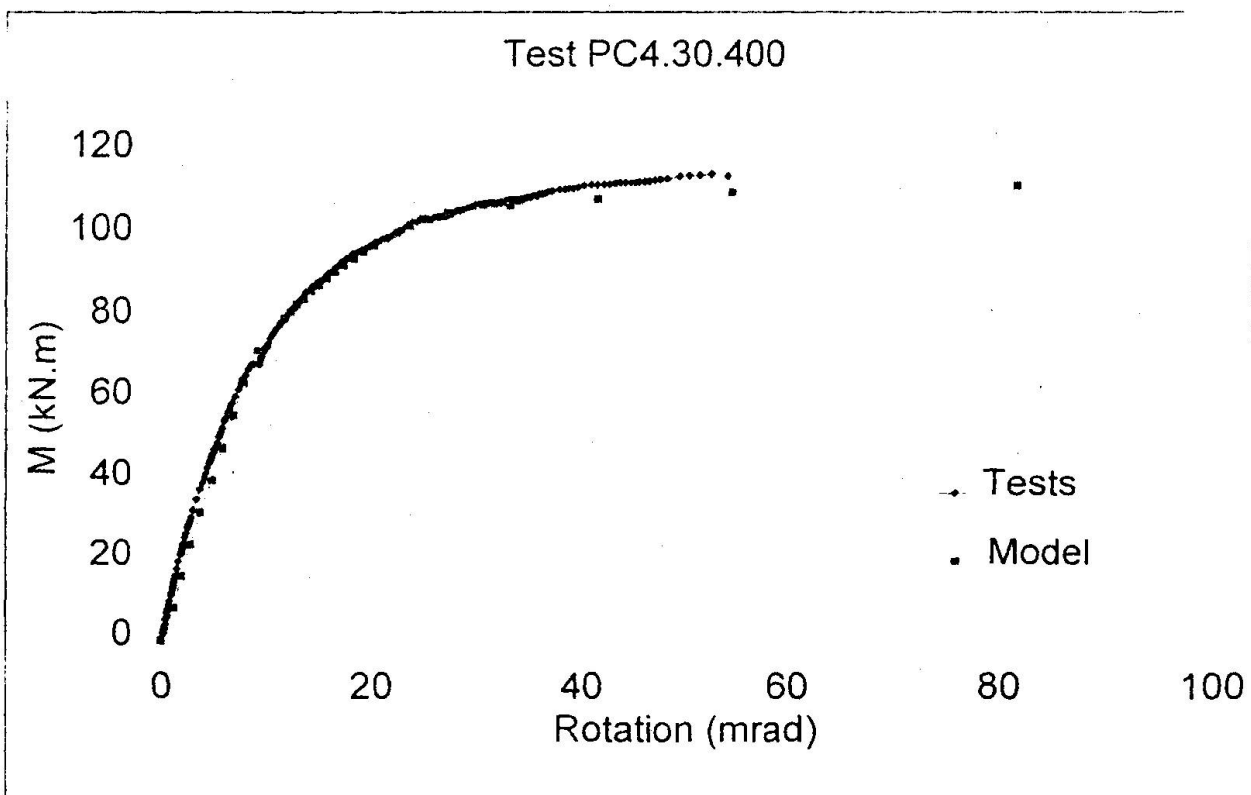
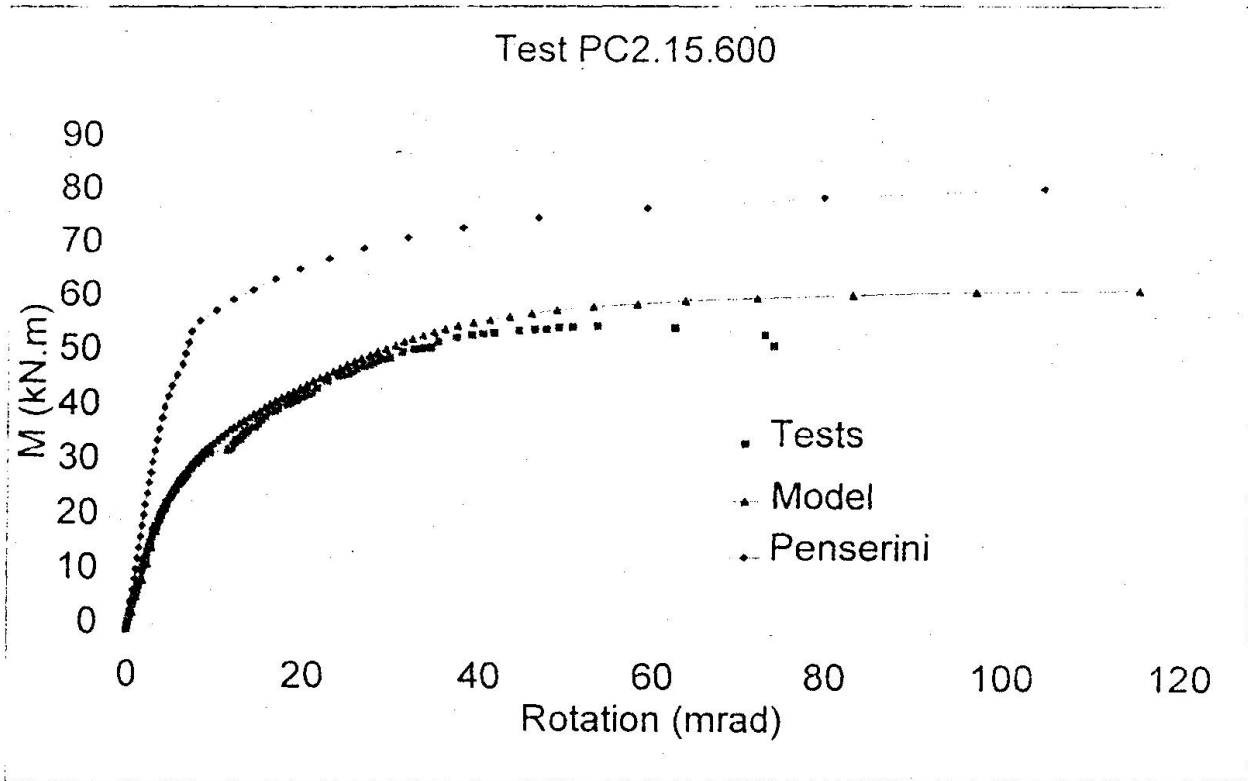


Fig. 6. Comparison between the model and the experimental curves



## 5. Comparisons with experimental tests

It is not possible to report on all the experimental tests in this paper. A full comparison can be found in the original research report [3]. Figure 6 shows the comparison for test PC2.15.600 and PC4.30.400.

In figure 6, the response predicted by the Penserini model [4] is also given for tests with two anchor bolts. The agreement between that model and the experiment is far from being satisfactory. It has however to be said that the tests considered here are outside the range of validity of the Penserini model.

For certain tests, some problems related to the execution has occurred (concrete, anchor bolts). Therefore, the comparison between those tests and the model was difficult. More details are given in [3].

As a conclusion to the full comparison, it can be stated that :

- For the tests with two anchor bolts, the initial stiffness is very well predicted by the model. The progressive yielding of the connection is also well covered by the theory.
- There are small discrepancies at ultimate state (5 to 10 %). This can be explained by the quite complex ultimate behaviour of the different connections components at ultimate state.
- Close to ultimate loading, the deformation of the column bases are quite important, this leads to modifications in the geometry, which are not taken into account in the model.

## 6. Conclusions

Experimental tests have been carried out on column bases with two or four anchor bolts. They have shown that the column bases have a very high semi-rigid behaviour, even for so called nominally pinned connections; this is known to be potentially beneficial when designing building frames.

A mechanical model is developed, based on the component method described in EC 3 Annex J. The non-linear behaviour of the different components is taken into account. Therefore, only an iterative procedure allows to describe correctly the connection behaviour for the whole loading. Furthermore, with such model, the history of the loading can be taken into account.

A comparison between the experimental curves and the model is given. The accuracy may be qualified as good, even if some small discrepancies occur at the ultimate state. Such a model is helpful in view of further investigations which would be aimed at developing a far more simple design procedure for practitioners.



## 7. References

- [1] EUROCODE 3 : Design of steel structure, part 1-1;  
General rules and rules for buildings, ENV 1993-1-1, 1992.  
Annex J : Joints in building frames, 1994.
- [2] EUROCODE 3 : Annex L : calcul and conception of column bases.
- [3] Guisse S. : Recherche COST C1; convention Région Wallonne, Université de Liège;  
sixième rapport semestriel : Extension des modèles de prédiction des courbes moment-  
rotation disponibles à Liège à d'autres types de noeuds poutre-colonne et aux  
assemblages en pied de colonne, 1995.
- [4] Penserini P., caractérisation et modélisation du comportement des liaisons structure  
métallique-fondation; thèse de doctorat de l'Université Pierre et Marie Curie,  
Paris 6, 1991.

Leere Seite  
Blank page  
Page vide



## Endplate and web plate joints: Moment–rotation behaviour

Vassili FRENKEL  
Mathematician

Vladimir KALENOV  
Civil Engineer, Dr.Sc.

Andrei PAVLOV  
Civil Engineer, Cand.Sc.

Sc. Res. Inst. Promstalkonstruktsiya  
Moscow, Russia

V. Frenkel, born 1949, graduated with a degree in mathematics from Moscow State University in 1971.

V. Kalenov, born 1942, graduated with a degree in civil engineer in 1964 from Moscow Civil Engineer University, he got his Cand.Sc. from Sc. Res. Inst. Proektstalkonstruktsiya, Moscow, in 1973, where he also earned a Dr.Sc. in 1995.

A. Pavlov, born 1959, graduated with a degree in civil engineer in 1982 from Moscow Civil Engineer University, where he also got a Cand.Sc. in 1987.

### Summary

The paper presents short description of methods and computer programs to determine “moment–rotation” characteristics of bolted beam–column joints with endplate and single/double web plate, which have been developed in Scientific Research Institute Promstalkonstruktsiya, Moscow. They are capable to calculate these types of joints taking into account any variation of geometrical and mechanical parameters of beams, columns and connection details. The calculation examples are also given.

### 1. Introduction

Traditionally the joints are considered as rigid or pinned at analysis of steel skeletons. However all joints possess definite bending strength, rigidity and deformativity. Consideration of these properties mutually enables to decrease the total weight of multistory steel structures up to 20%. To describe the behaviour of joints the correlations between the bending moment transmitted by the joint ( $M$ ) and its rotation ( $\phi$ ) are usually used. The works on investigation and determination of  $M$ – $\phi$  characteristics of beam–column joints of different types are being provided now in Scientific Research Institute Promstalkonstruktsiya, Moscow. This paper is devoted to definition of  $M$ – $\phi$  characteristics of joints with endplate and single/double web plate.

### 2. Endplate joints

#### 2.1. General part

The theoretical model of endplate joints behaviour takes into account 9 endplate types, which are shown in *Fig. 1*. Columns can be strengthened by stiffeners. Bolts can be pretension.

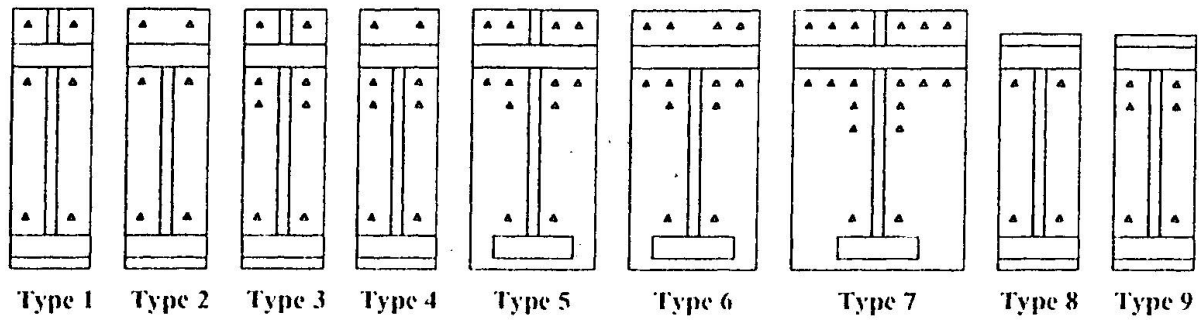


Fig. 1. Endplate types.

Shown in Fig. 2 the "moment-rotation" characteristic is produced with the formula proposed by Chen and Kishi [1]

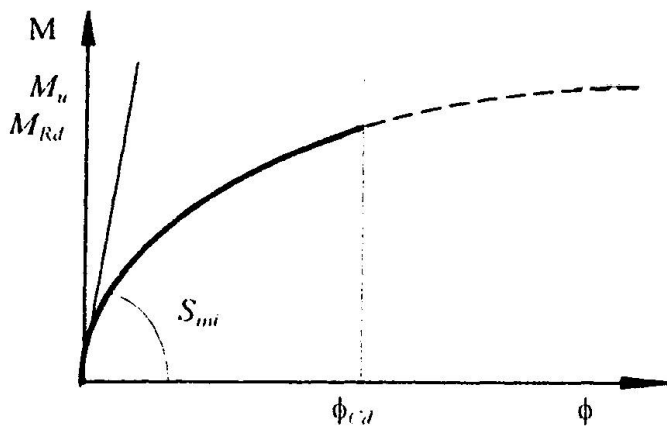


Fig. 2. "Moment-rotation" characteristic.

$$M = \frac{S_{mi} \phi}{\left[ 1 + \left( \frac{S_{mi} \phi}{M_u} \right)^{1.8} \right]^{0.56}} \quad (1)$$

$$\phi_{cd} = \frac{M_u M_{Rd}}{S_{mi} (M_u^{1.8} - M_{Rd}^{1.8})^{0.56}} \quad (2)$$

$S_{mi}$  – initial stiffness

$M_u$  – ultimate moment capacity

$M_{Rd}$  – design moment resistance

$\phi_{cd}$  – design rotation capacity

The partial safety factors are taken equal to 1,0 for the ultimate moment capacity calculation and equal to their real values for design moment resistance calculation.

The parameters calculation of formulac (1) and (2) is produced for the total loadintroduction "TL" (for points PL and PC in Fig. 3), the column web in shear "s.wc" (for points PS and PC in Fig. 3) and total joint "TJ" (for point PC in Fig. 3).

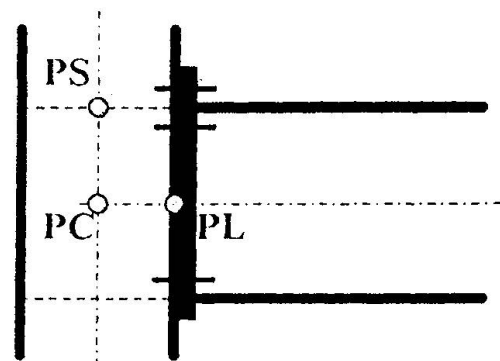


Fig. 3. Points definition according [2].

## 2.2. Total loadintroduction

### 2.2.1 Initial stiffness

$S_{TL,mi,PL}$  is calculated by the computer program "Flora" which is based on the elastic finite element model of endplate joints. The column flange and the endplate represent two independent plates divided to finite elements. The bolts are the internal constraints between the

column flanges and the endplates finite element nodes. Bolt pretension is accepted. The column web and stiffener behaviour is simulated by the constraints in the column flange on its connection line with the column web and stiffener.

$$S_{TL,ul,IV} = \frac{S_{j,b} S_{TL,im,PL}}{S_{j,b} - S_{TL,im,PL}} \quad (3)$$

$$S_{j,b} = 2EI_b/h_c \quad (4)$$

### 2.2.2 Strength

Ultimate moment capacity and design moment resistance are defined as minimal bending moment which is necessary to apply to the joint to obtain the limit state in one of its elements. The following limit states for the total joint are considered:

- crushing forces achievement in maximally loaded bolts if moment  $M_{b,u}$  or  $M_{b,Rd}$  acts;
- plastic hinge propagation into the endplate if moment  $M_{ep,u}$  or  $M_{ep,Rd}$  acts;
- plastic hinge propagation into the column flange if moment  $M_{fc,u}$  or  $M_{fc,Rd}$  acts;
- yield stresses achievement in the part of column web subjected to local tension if moment  $M_{l,wc,u}$  or  $M_{l,wc,Rd}$  acts;
- yield stresses achievement in the part of column web subjected to local compression or column web buckling if moment  $M_{c,wc,u}$  or  $M_{c,wc,Rd}$  acts.

$$M_{TL,u,PL} = M_{TL,u,IV} = \min\{M_{b,u}, M_{ep,u}, M_{fc,u}, M_{l,wc,u}, M_{c,wc,u}\} \quad (5)$$

$$M_{TL,Rd,PL} = M_{TL,Rd,IV} = \min\{M_{b,Rd}, M_{ep,Rd}, M_{fc,Rd}, M_{l,wc,Rd}, M_{c,wc,Rd}\} \quad (6)$$

## 2.3. Column web in shear

### 2.3.1 Initial stiffness

$S_{s,wc,im,PS}$  is calculated by the traditional methods of the theory of elasticity.

$$S_{s,wc,im,IV} = \frac{S_{j,c} S_{s,wc,im,PS}}{S_{j,c} - S_{s,wc,im,PS}} \quad (7)$$

$$S_{j,c} = 4EI_c/h_j \quad \text{-- Internal and End Joints} \quad (8)$$

$$S_{j,c} = 2EI_c/h_j \quad \text{-- T and Knee Joints} \quad (9)$$

### 2.3.2 Strength

Ultimate moment capacity  $M_{s,wc,u,PS} = M_{s,wc,u,PC}$  and design moment resistance  $M_{s,wc,Rd,PS} = M_{s,wc,Rd,PC}$  are defined using the proposals of Innsbruck University [3].

## 2.4. Total joint

### 2.4.1 Initial stiffness

$$S_{TL,im,IV} = \frac{S_{TL,im,IV} \cdot S_{s,wc,im,IV}}{S_{TL,im,IV} + S_{s,wc,im,IV}} \quad (10)$$

### 2.4.2 Strength

$$M_{TL,u,IV} = \min\{M_{TL,u,IV}, M_{s,wc,u,IV}\} \quad (11)$$

$$M_{TL,Rd,IV} = \min\{M_{TL,Rd,IV}, M_{s,wc,Rd,IV}\} \quad (12)$$



## 2.5. Used formulae

All used formulae are included in the documentation of the International Module Bank System, developed at the Institute of Steel and Timber Construction, University of Innsbruck.

## 2.6. Computer program

The computer program is aimed for the determination of "moment-rotation" characteristics of endplate joints and connected to the International Module Bank System as Module No. 3 MOS\_EP [4]. Program output data are:

- values of the initial stiffness', the ultimate moment capacities, the design moment resistances and the coordinates of the relationships "moment-rotation" for total joint and separately for shear panel and total load introduction;
- characteristic points of the beam line for the condition of yield stresses constant level;
- coordinates of a intersection point of "moment-rotation" curve with beam line (support moment and rotation);
- value of the related load  $q_{rel}$  [5] demonstrating how much times the load taken up by the beam with chosen joint exceeds the load taken up by the same beam with pinned supporting (the uniformly distributed load is considered).

## 2.7. Calculation example

### 2.7.1. Joints characteristics

Ten endplate joints with the following characteristics have been chosen for calculation:

- beam 55B2 ( $h_b=547$  mm,  $b_b=220$  mm,  $t_{fb}=15.5$  mm,  $t_{wb}=10.0$  mm,  $r_b=24$  mm) with the span  $l_b=6$  m and 12 m;
- column 30C1 ( $h_c=296$  mm,  $b_c=300$  mm,  $t_{fc}=13.5$  mm,  $t_{wc}=10.0$  mm,  $r_c=18$  mm);
- steel of beam, column, backing plates and column stiffeners S255 ( $f_y=245$  Mpa,  $\gamma_{M0}=1.025$ );
- endplates steel S390 ( $f_y=390$  MPa,  $\gamma_{M0}=1.025$ );
- bolts: diameter M24, high strength ( $f_u=1100$  MPa,  $\gamma_{MB}=1.43$ ).

Endplate dimension are shown in Fig. 4, thickness' of endplate ( $t_{ep}$ ), column stiffeners ( $t_{st}$ ), backing plates ( $t_{bp}$ ) and bolt pretension efforts ( $B_p$ ) are presented in Table 1.

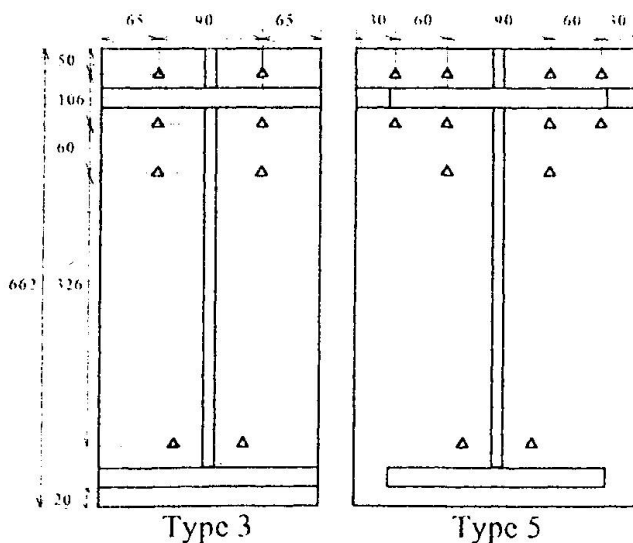


Fig. 4. Endplate dimension.

No	Type	$t_{ep}$ mm	$t_{st}$ mm	$t_{bp}$ mm	$B_p$ kN
1	3	25	16	16	239
2	3	16	10	10	239
3	3	25	16	16	–
4	3	16	10	10	–
5	3	25	–	–	–
6	5	25	16	16	239
7	5	20	10	10	239
8	5	25	16	16	–
9	5	20	10	10	–
10	5	25	–	–	–

Table 1. Selected characteristics of endplate joints elements.

### 2.7.2. Calculation results

The values of initial stiffness, design moment resistances and related loads of all numerical tests are presented in *Table 2*.

N	$S_{II,ini,PL}$	$S_{s,wc,ini,PS}$	$M_{b,Rd}$	$M_{cp,Rd}$	$M_{jc,Rd}$	$M_{l,wc,Rd}$	$M_{c,wc,Rd}$	$M_{s,wc,Rd}$	$q_{rel}$	$q_{rel}$
	kNm/rad	kNm/rad	kNm	kNm	kNm	kNm	kNm	kNm	$l_b=6m$	$l_b=12m$
1	500000	203698	556	1690	1060	965	846	1526	1,54	1,45
2	377358	168242	538	688	667	743	604	1034	1,66	1,49
3	168067	203698	556	1690	1060	965	846	1526	1,89	1,63
4	148148	168242	538	688	667	743	604	1034	1,78	1,76
5	111111	109147	556	1690	333	374	255	216	1,40	1,32
6	512821	203698	851	1896	1005	965	846	1526	1,70	1,60
7	465116	168242	801	1211	634	743	613	1034	1,97	1,90
8	253165	203698	851	1896	1005	965	846	1526	1,90	1,70
9	229885	168242	801	1211	634	743	613	1034	1,88	1,97
10	116279	109147	851	1896	310	374	255	216	1,40	1,29

*Table 2. Endplate joints calculation results.*

The corresponding total load introduction “moment–rotation” curves for point PL are shown in *Fig. 5*.

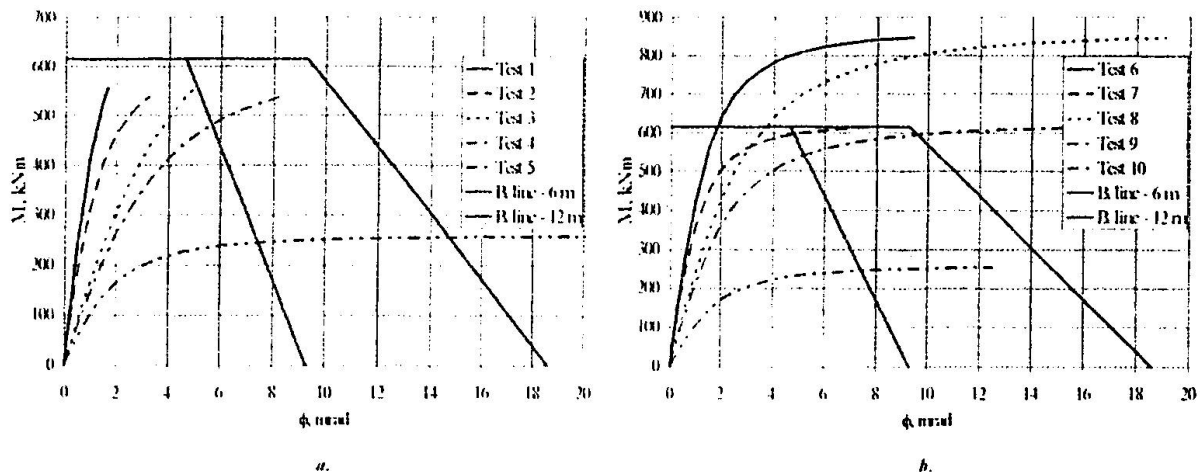


*Fig. 5. Total load introduction endplate joints “moment–rotation” curves for point PL: a) tests 1 – 5, b) tests 6 – 10.*

Present examples demonstrate the efficiency of endplate joints with four vertical rows and pretension bolts.

## 3. Single/double web plate joints

### 3.1. Description of algorithm and computer program

The theoretical algorithm to determine the “moment–rotation” characteristics is developed on the base the investigation of real behaviour of joints. The main consumption into deformativity



of joints is made by the deformations of mutual rotation between connected elements. These deformations take place because of the bolts bearing and bending, the connected elements bearing, the beam slippage relatively to the plate when the tolerances between the bolts and the holes are available.

The determination of "moment-rotations" characteristics which characterize mutual rotation of connected elements is obtained by the computer program SDVIG. The main principles of the analytical model which is used in the program are:

- the displacements  $\delta_i$  of the beam web points relatively to the plate are proportionally to their distance to the rotation center  $r_i$ ;
- the respective forces  $N_i$  taken up by the bolts and the connected elements are obtained with the help of real non-linear curves "force-displacement" defined from the tests of single-bolts connections subjected to shear;
- moment  $M$  taken up by the joint is defined as sum of moments  $M_i$ , taken up by each couple of bolts symmetrically arranged relatively to rotation center:  $M = \sum M_i = \sum N_i r_i$ ;
- specified successive steps for gradual increase of rotation it is executed the calculation of the according moments values.

It is necessary to point out that the presented model contains principally new approach to determine the forces distribution between the bolts in the connection comparatively to the traditional approaches. These traditional methods consider that the forces taken up by the bolts is distributed between them proportionally to distance from their rotation center. In proposed method the bolt forces are defined depending upon the real displacements of the connected elements in the places where the bolts are installed.

Program SDVIG input data are: Russian and European beam profiles; plate thickness; steel of beam and plate; number of plates; number of bolt rows; number of bolts per row; dimension of connection; bolts grade - high strength, 10.9, 8.8 or 5.8; bolts diameter - M24 or M20; holes diameter; beam length; maximum rotation and number of steps. Output data of the program SDVIG are the same one of the program MOS\_EP.

### 3.2. Calculation example

Six single web plate joints with the following characteristics have been chosen for calculation:

- beam 80B1 ( $h_b=791$  mm,  $h_p=280$  mm,  $t_{pb}=17.0$  mm,  $t_{wb}=13.5$  mm,  $r_b=26$  mm) with the span  $l_b=6$  m and 9 m;
- beam steel S345-3 ( $f_y=320$  MPa,  $\gamma_{M0}=1.025$ );
- web plate ( $t_p = 20$  mm, 18 mm, 16 mm, 14 mm, 12 mm, 10 mm);
- web plate steel S255 ( $f_y=245$  MPa,  $\gamma_{M0}=1.025$ );
- bolts: diameter M24, high strength ( $f_u=1100$  MPa,  $\gamma_{MB}=1.43$ );
- holes diameter 27 mm.

This calculation example shows that the changing of the web plate thickness can provide the best combination of joint strength and deformativity which give an opportunity for the structure to take up the maximal load. Fig. 6 shows "moment-rotation" curves of the joint with different plate thickness'. The values of relative loads  $q_{rel}$  for the beam with the spans 6 m and 12 m are presented in Table 3.

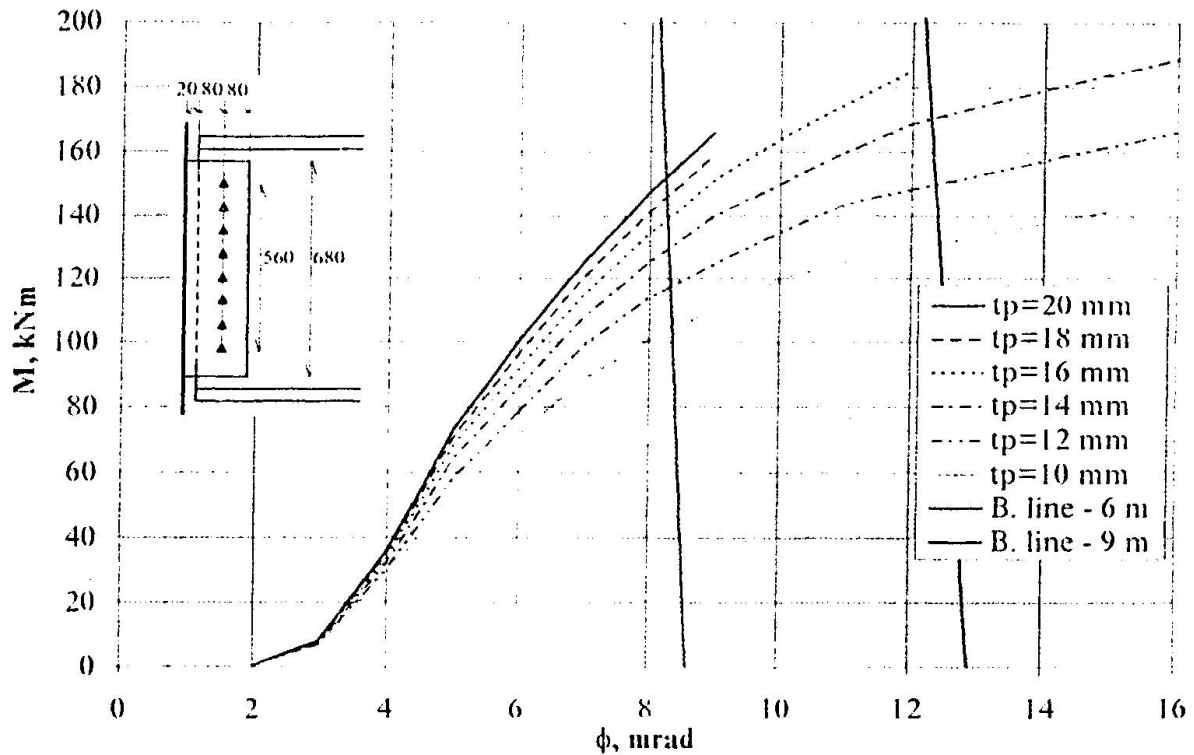


Fig. 6. "Moment-rotation" curves of single web plate joint.

Beam span, m	Plate thickness, mm					
	20	18	16	14	12	10
6	1,084	1,081	1,077	1,072	1,065	1,058
9	0,833	0,827	1,081	1,094	1,083	1,073

Table 3. Relative loads values.

Fig. 6 and Table 3 analysis has got clear that the web plate of 20 mm thickness is the most effective ( $q_{rel}=1,084$ ) for the structure with 6 m beam span. However its use at the beam with the span 9 m is wrong because the joint gets up no enough flexible in this case. Value of relative load is  $q_{rel}=0,833$  or the permitted load applied to the beam with real supports is 16% less than to the same one with pinned connections. Decreasing the plate thickness or increasing the flexibility of the joint demonstrates that the web plate of 14 mm thickness is the most useful for the structure with 9 m beam span ( $q_{rel}=1,094$ ).

#### 4. Comparison with the test results

There is a good correspondence between the calculation methods of endplate and single/double web plate joints and the experimental results. The Russian tests, concerning the mentioned joints, are included to the International Data Bank SERICON [6] (tests 110.001 – 110.009, 111.001 – 111.014).



## 5. Conclusion

In this manner the calculation methods and computer programs to determine “moment–rotation” characteristics of T–stub and top and seat angle joints have been developed. “Moment–rotation” curves of the joints have been used for the global analysis of the building steel skeletons. The total steel weight was decreased up to 15–20% relatively to the results obtained by the traditional frame design.

## References

- [1] CHEN, W.F.; KISHI, N. *Moment–Rotation of Semi-Rigid Connections*, Structural Engineering Report, No 7, Purdue University, West Lafayette, 1987.
- [2] TSCHEMMERNEGG, F.; HUBER, G. *Joint Transformation and Influence for the Global Analysis*, COST–C1/ECCS TC11, Drafting Group for Composite Connections, Technical Paper T6, 1995.
- [3] ÖSTV. *Rahmentragwerke in Stahl*, Österreichischer Stahlbauverband, 1987.
- [4] SCHAUR, B.C. *Entwicklung einer Modulbank für Stahl- und Verbundknoten*, Dissertation am Institut für Stahlbau und Holzbau der Universität Innsbruck, 1995.
- [5] PAVLOV, A. *Determination of Efficiency of Beam-to-Column Joints*, The 9-th. International Conference “Metal Structures”, Proceedings, Krakow, 1995.
- [6] HUTER, M. *Data Bank Program SERICON – Development in Innsbruck*, COST C1 Workshop, Prague, 1994.



## Effect of Bolt Modeling on Initial Stiffness of Cleated Connections

**Kemal Burak HANOĞLU**  
Research and Teaching Assistant  
Department of Civil Engineering  
Boğaziçi University  
Bebek, İstanbul  
TURKEY

Kemal Burak Hanoğlu  
received his B.Sc. in Civil Engineering in 1994  
and M.Sc. in Civil Engineering in 1996  
from Boğaziçi University.

**Gülay Altay AŞKAR**  
Professor and Head of Department  
Department of Civil Engineering  
Boğaziçi University  
Bebek, İstanbul  
TURKEY

Gülay Altay Aşkar  
received her Ph.D. in Civil Engineering in 1977  
from İstanbul Technical University.  
Head of Civil Engineering Department since 1992  
and Vice Dean of Engineering Faculty since 1995  
at Boğaziçi University.

### Summary

Finite element models of semirigid cleated connections are used to evaluate the contribution of the bolts to the connection initial stiffness. Two dimensional shell and one dimensional bar elements are used to construct the models and the three dimensional behavior of the connection is thereby approximated. Bolt to plate contact regions and bolt heads and nuts are included in the finite element models using local modeling details called *bolt models*. Results are compared with test results and analytical formulae in the literature.

### 1. Connection Models

Three types of cleated connections are investigated using finite element models, six *top and seat angle with double web angle* connections, and as their subassemblies with same geometrical and material properties, five *top and seat angle* and three *double web angle* connections. The dimensions of the modeled *top and seat with double web angle connections* are taken same as in the static test series performed by Azizinamini *et al.* (1989), Table 1.

#### 1.1. Modeling Assumptions

Material is assumed to behave linear elastic, isotropic and homogeneous in the load range of interest. To enable direct comparison with the results of analytical formulae, Azizinamini *et al.* (1989) and Kishi *et al.* (1990), the contributions of the column flanges and web to the flexibility of the connection are neglected. Thus, the column flange is replaced with a *rigid boundary*. At the initial stage of the loading the applied forces on the connection are small compared to the applied bolt pretension force. Therefore, the effect of pretension in the vicinity of bolts is modeled using deformational constraints. Due to the symmetry of the above mentioned connection types only the half of the connections are modeled.



Table 1. Properties and Test Results of Azizinamini et al. (1985) Test Series.

(a) Top and Seat with Double Web Angle Connections

Test ID Number	Bolt Diameter $\varnothing$ (mm.)	Average Nut thickness $H_a$ (mm.)	Web angle thickness $t_{ww}$ (mm.)	Top & seat thickness $t_{ts}$ (mm.)	Test Results $k_{i,exp}$ [kN-m/rad]
14S1	19.1	15.3	6.4	9.5	22035
14S2	19.1	15.3	6.4	12.7	33335
14S4	19.1	15.3	9.5	9.5	25075
14S5	22.2	17.9	6.4	9.5	27911
14S6	22.2	17.9	6.4	12.7	32318 *
14S8	22.2	17.9	6.4	15.9	65427

(b) Top & Seat Angle Connections

Model ID	Bolt Diameter $\varnothing$ [mm]	Average Nut thickness $H_a$ [mm]	Top & seat thickness $t_{ts}$ [mm]
TS1	19.1	15.3	9.5
TS2	19.1	15.3	12.7
TS5	22.2	17.9	9.5
TS6	22.2	17.9	12.7
TS8	22.2	17.9	15.9

(c) Double Web Angle Connections

Model ID	Bolt Diameter $\varnothing$ [mm]	Average Nut thickness $H_a$ [mm]	Web angle thickness $t_{ww}$ [mm]
DW1	19.1	15.3	6.4
DW4	19.1	15.3	9.5
DW5	22.2	17.9	6.4

\* Same configuration under the name 14S9 has  $S_i=29154$  kN-m/rad, Azizinamini et al. (1985).

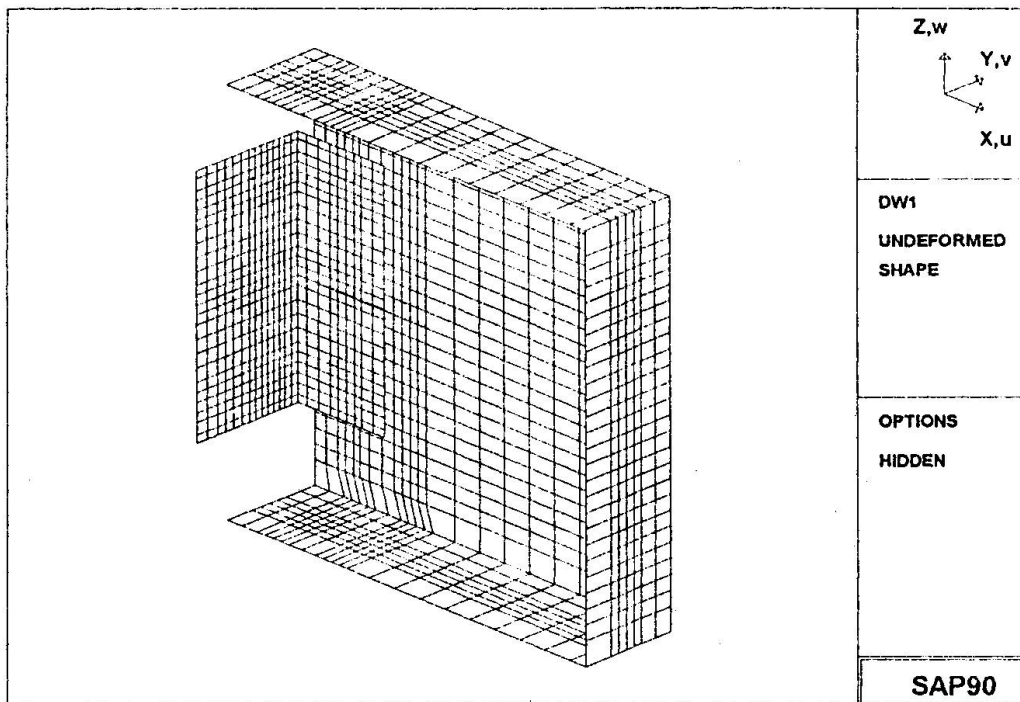


Figure 1. Sample Finite Element Mesh for Double Web Angle Connections.

## 1.2. The Model

Connection models include a portion of the beam of a length equal to the depth of the profile, and the other components such as the cleats, bolts and nuts. Moreover, a rigid plate is attached to the end of the beam portion. Loads are applied onto this plate to avoid stress concentrations on the finite elements forming the beam profile and connection components, Figure 1.

The portions of the cleats and connectors in contact with the column flanges are forming the *column boundary*. The portions of plates or cleats in the connection in contact with the beam are forming the *plate boundary*.

### 1.2.1. Discretization

Beam profile and cleats are discretized using four noded quadrilateral shell elements with plate bending and stretch capabilities. The shell element layers are located at the midheight of the web and flanges of the I-profile, and the legs of the cleats. The shell element layers are assigned the corresponding thickness of the modeled regions. Bolt shanks are formed using bar elements and the ends of the bars are connected to the shell element layers. The ends of the bar elements are released with respect to torsion.

Bolt heads and nuts are represented in the finite element models in two different ways. Either these portions are assumed to impose certain constraints on the deformation of the shell layers, and this is modeled with restraints and/or constraints, or an additional patch of shell elements is placed onto the shell layers that are already formed for cleat legs or I-profile plates. These sets of restraints and/or constraints, or element patches are named as *bolt models*. The *bolt models* are applied at each bolt location in the model.

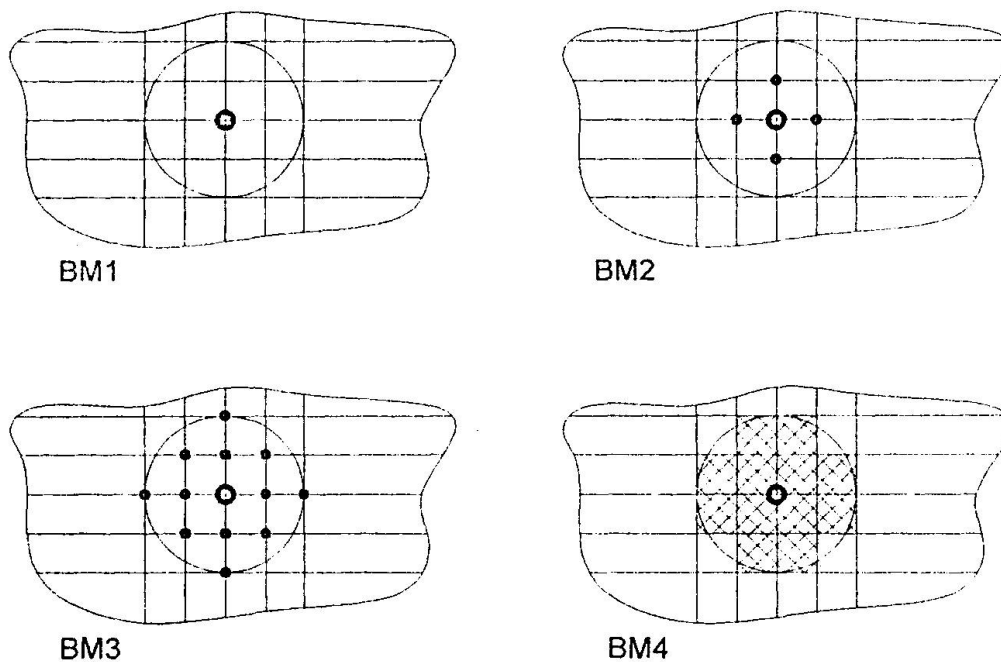


Figure 2. Bolt Models.

### 1.2.2. Bolt Models

There are four *bolt models*; BM1, BM2, BM3 and BM4. In Figure 2., the implications of the applied *bolt models* are indicated on corresponding sketches. Intersection points of the lines are the active nodes of the model. A bolt element end node is identified with a thick ring. The true diameter of the bolt head or nut is shown with a thin circle, and it is taken equal to the distance across flats of the bolt head. A heavy dot in these sketches stands for a constraint to be applied to the marked node. This constraint forces the marked node to translate equally with a node on another mesh layer that is adjacent to this node. For example, this case arises for the bolts connecting the cleats to the beam profile flanges. In this and similar regions, two mesh layers are adjacent to each other with same mesh density and they are formed so that the projection of their nodes onto the horizontal plane coincide.

The first three *bolt models* aim to define the radius of influence of the bolt heads and nuts. This is achieved by increasing the radius of the restrained and constrained region around the bolt element end nodes. Bolt model BM1 is a configuration where no stiffening effect due to the presence of bolt head and nuts nor due to pretension is modeled. BM2 has the restraint and constraint sets applied at the first neighbourhood of the bolt end nodes only. Therefore, only the nodes on the shell layers that are belonging to the bolt shank are influenced. This corresponds to a better representation of the bolt shank. BM3 applies the maximum number of restraints, that is to all of the nodes inside the bolt head diameter. This results in the full restraint of the nodes in this region and models the presence of pretensioning.

Bolt model BM4 is using an additional shell element patch to model the stiffness of the bolt head and nut.

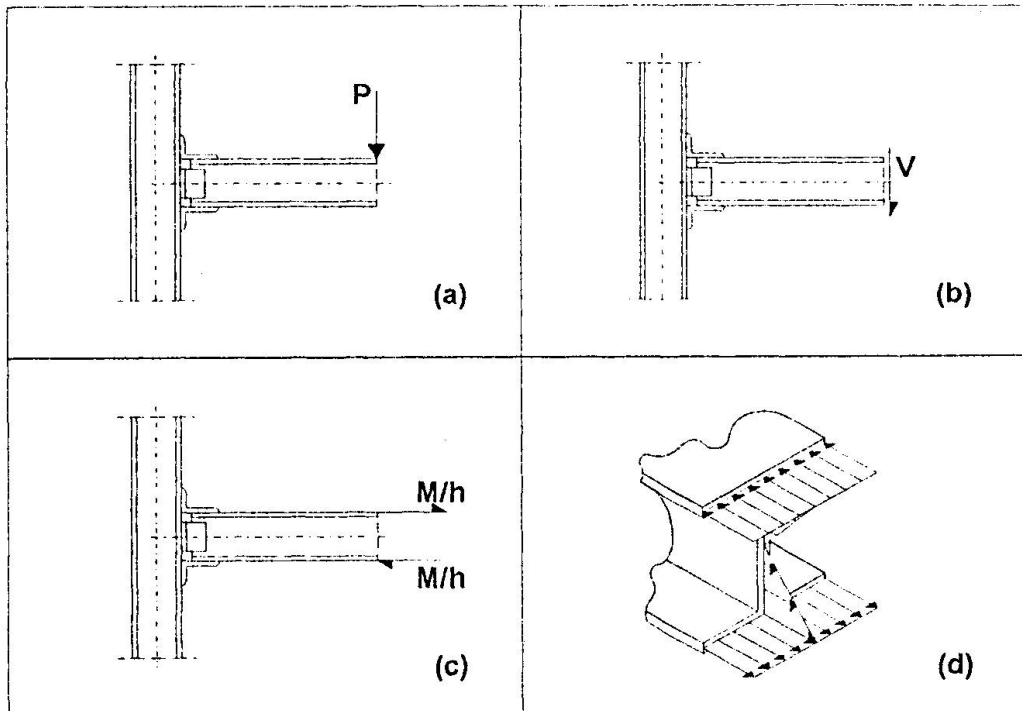


Figure 3. Possible Loading Cases.

### 1.3. Loading

As a part of a frame, connections may be subjected to direct shear, eccentric shear, which produces a combination of direct shear and a twisting moment, direct tension, moment and combinations of these cases. Possible loading cases of finite element models are shown in Figure 3. Without the load application plate all loading cases except (d) cause stress concentrations and improper stress boundary conditions for the beam free end. Loading case (d) represents linear stress distribution throughout the cross section implying pure bending of the member, Krishnamurthy *et al.*, 1976, and Sherbourne *et al.*, 1994.

The connection specimens subject to testing are often statically determinate subassemblies, tested under point loading. With the dimension information of the subassembly provided, the moment, shear and axial force values at the location of the load application plate can be calculated and applied as statically equivalent concentrated loads acting on the load application plate. Thus a combined loading made of shear and moment that is representative of the loading during testing is obtained, case (b) and (c).

### 1.4. Computational Methodology

The finite element program, SAP90 is verified for convergence performance by solving benchmark plate bending and stretch problems with different mesh densities. The results indicate that the calculated nodal displacement values are uniformly converging to the exact solutions of the posed benchmark problems. With increase in the number of nodes and elements used in the model the deformations increase and approach the exact value asymptotically. Therefore, convergence of the finite element analysis results is provided with the refinement of the finite element model mesh.



A connection is first analyzed with the only constraint applied by the bolts connected at the *column* and *plate boundaries*. This analysis results in incompatibility at all the contact regions. As an example, cleats on the *column boundary* penetrate into the column flanges. *Rigid boundary* to element mesh contact locations are defined applying a sequence of analysis and control of boundary violation. Incompatibilities at the boundaries are detected and the locations of these penetrations are listed and sorted regarding the magnitude of deformation. These penetrations are prevented applying restraints to the relevant deformational degrees of freedom of the nodes. For restraining purposes, groups of nodes of maximum violation are selected so that the first and last selected nodes do not significantly differ in the magnitude of their deformation. A maximum number of 20 nodes is used in restraining. Analysis and control are continued until no violation in the contact boundaries are left. Five to seven iterations are needed to achieve convergence of boundary contact conditions.

For the initial stiffness calculation the output of only two nodes is used. These are the nodes that are at the beam end and at the mid height of the flanges. Moreover, the difference between the Y- and Z- displacements,  $\Delta v$  and  $\Delta w$ , are not included in the calculation of rotation, Krishnamurthy *et al.*, (1976). Thus, the angle  $\theta$  is obtained by dividing the difference of the X- displacements,  $\Delta u$ , of the flange centroids by the distance between these points. Inverse of this value multiplied by the applied moment,  $M_f$ , yields the required initial stiffness. Errors in prediction of initial stiffness results are evaluated taking the test results and analytical models reported in references as basis.

## 2. Finite Element and Analytical Modeling Results of Cleated Connections

For the modeling study of cleated connections, a well documented and frequently referred test series is selected as reference (Azizinamini *et al.*, 1989). Specimens of the test series consist of two beam sections attached to a stub column that is positioned between these two beams and connected to them by *top and seat angle with double web angle connections*. The specimens are simply supported at the beam free ends and loaded through the column by an applied point load to a plate attached to the top of the column. The described configuration is statically determinate. Therefore, simple statics may be used to determine the moment and shear composition at any distance away from the column face to determine the actual loading composition that was present during early stages of the test.

### 2.1. Finite Element Model Results

Figure 4. summarizes the results for the modeled six *top and seat angle with double web angle connections*. In the test series results of two specimens with identical properties, numbered as 14S6 and 14S9, have been reported, only the test and finite element modeling results of specimen 14S6 are reported herein.

For the investigation of *double web angle (DW)*, and *top and seat angle connection (TS)* behavior, the specimens of the above mentioned test series are separated into connections having the same cleats and gages used in the test series with only top and seat angles or web angles.

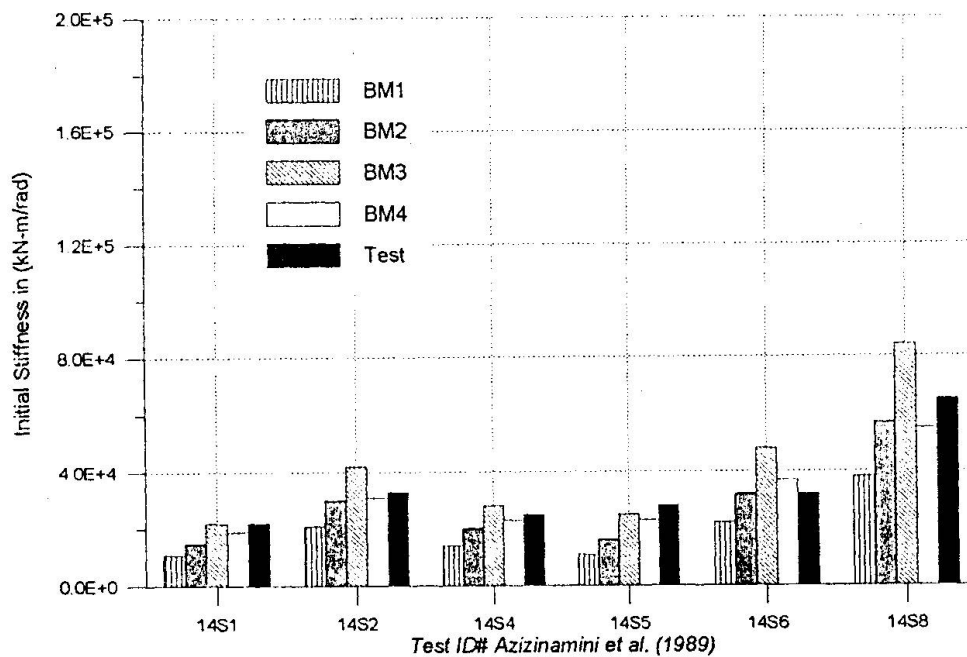


Figure 4. Finite Element and Test Results for Top and Seat with Double Web Angle Connections.

## 2.2. Analytical Model Results

Analytical models for the initial stiffness of cleated connections have been presented by Kishi *et al.* (1990 and 1993), assuming that the center of rotation is located at the heel of the seat angle bearing to the column. This model implies the superposition of the models separately derived for *top and seat angle connections*, and *double web angle connections*.

In the study by Azizinamini *et al.*, the tension flange and web angles are modeled as assemblies of "beam" segments and their individual contribution to the total stiffness of the connection are calculated. This model is calibrated with the deformation pattern observed during the tests. Two sets of expressions for the initial stiffness of *top and seat angle with double web angle connections* are presented with and without shear deformations of the "beam" segments.

The initial stiffness values calculated or reproduced using the above stated references are given in the Figure 5-7. These figures include a comparison made using the finite element model results of BM4. The test results for *top and seat with double web angle connections* are also included in Figure 5.

## 2.3. Comparison of Finite Element and Analytical Model Results

The analytical models use a simplified distribution of applied loads and assume a single contact condition that is assumed to be valid for all possible gage and thickness configurations. Furthermore, superposition principle is used to form the more complex connection geometries using the subconnection deformations and stiffnesses. Therefore, where one of the above given simplifying assumptions are not applicable, the results tend to deviate from the test results. This

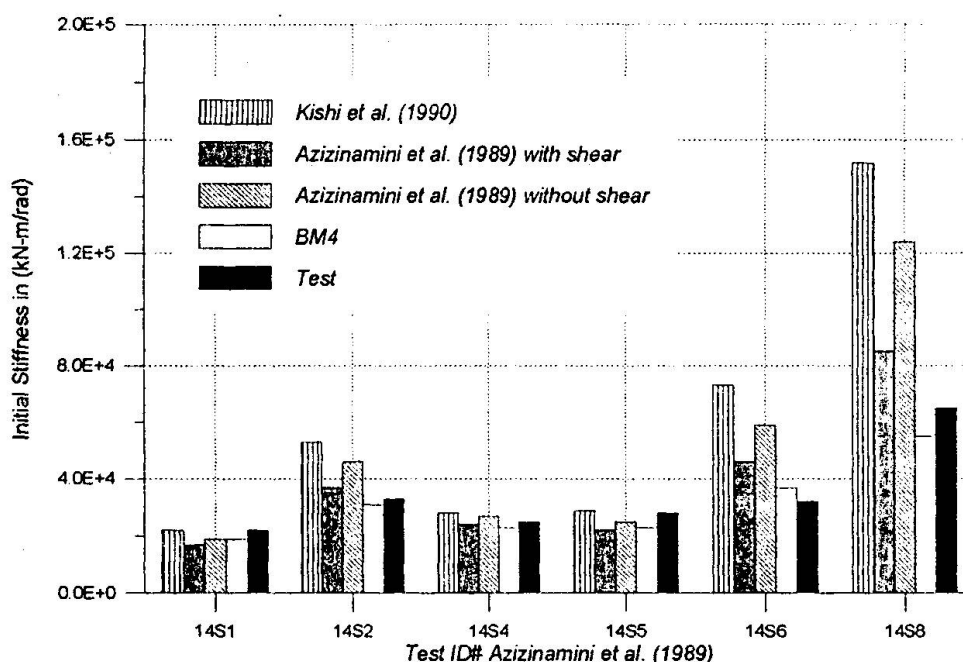


Figure 5. Initial Stiffness Results for Top and Seat with Double Web Angle Connections.

is particularly obvious for top and seat with double web angle connection configurations with thick top and seat angles where the analytical formulae over estimate the connection stiffness.

With reference to the test results, the finite element models have produced satisfactory results. Finite element results are obtained using a standardized procedure to provide repeatability and are, therefore, applicable to all connection geometries. In finite element modeling, the loading is made to resemble to the actual loading applied during testing and the contact conditions are defined using iterative schemes.

### 3. Conclusions

Connections modeled in this study cover a wide range of cleated semirigid connection types. Modeled portion of the connection includes a portion of the connected beam that is of one beam depth length and all of the connectors and secondary elements. Column flange and web are not modeled. This allowed direct comparison of finite element modeling performance with analytical models that exclude the column flange and web stiffness, and tests that are performed using stiff columns. Moreover, the behavior of the connectors and secondary elements can be observed more closely this way. The finite element models are constructed and analyzed using a unified modeling approach. Two and one dimensional finite elements are used to approximate the three dimensional behavior of the connections. Thereby, saving on computation time is achieved. The assumptions made in the modeling of connections are supported by the observed behavior reported by the researchers working in this field. Initial attempts on modeling indicated that there are three major sources of stiffness contribution other than the stiffness of secondary elements in the connection. These are local effects such as, stiffening effect of bolt heads and nuts, friction between the connected components and pretensioning of bolts. These conclusions resulted in the development of *bolt models*.

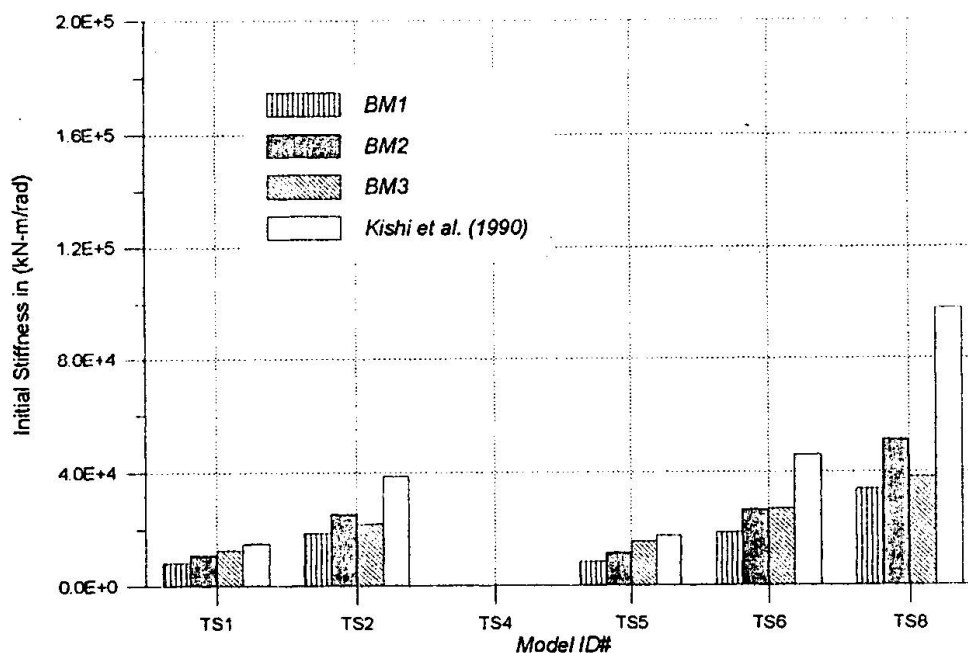


Figure 6. Initial Stiffness Results for Top and Seat Angle Connections.

The *bolt models* (BM) comprise of restraint and constraint patterns that model the influence of the pretension and account for the presence of the bolt heads and nuts. With the *bolt models*, it is possible to represent, non-pretensioned bolted connections accounting for the presence of bolt heads and nuts (BM4), and different levels of pretension (BM2 and BM3). Also a lower bound for the connection stiffness is established (BM1) with no allowance made for the presence of bolt heads and nuts nor for pretensioning forces.

For cleated connections the mechanism of deformation is related to the deformation of the cleats rather than the local deformations of the secondary connection elements. The presence of bolt heads and nuts are equally important as the application of the pretensioning forces. The element patches used in BM4 produce the same effect as the sets of restraints, except in cases of thick angles where BM4 performs better. This suggests that there is a relation between the bolt head thickness and the thickness of the connected angle. For thin angles the bolt heads fully dominate the behavior and this is evident of the closeness of the results of BM3 and BM4. However, if the angle thickness increases, the bolt heads cannot force the angles to remain in contact as in the other case. This is seen in over estimation of the BM3 and is supported by the proper prediction of BM4.

Finite element modeling results indicate the importance of correct modeling of the stiffness sources and contact conditions. This can be seen in the difference of the results among *bolt models*. Analytical models presented in the literature involve assumptions that are not justified by the observed behavior of the connections. This results in erroneous initial stiffness prediction. The assumptions that are of major importance are those related to contact boundary conditions. Therefore, any other assumption violating these conditions is also invalid.

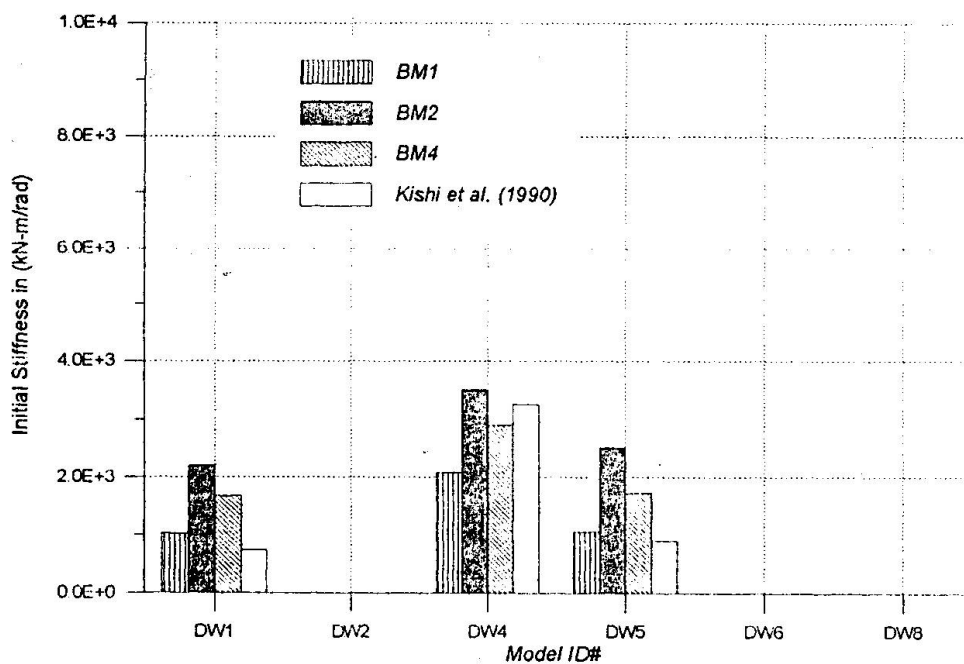


Figure 7. Initial Stiffness Results for Double Web Angle Connections.

## References

- Azizinamini, A., and J. B. Radzimirski, "Static and Cyclic Performance of Semirigid Steel Beam-to-Column Connections," *Journal of Structural Engineering*, ASCE, Vol. 115, No. 12, pp. 2979-2999, December, 1989.
- Kishi, N., and W-F. Chen, "Moment-Rotation Relations of Semirigid Connections with Angles," *Journal of the Structural Division*, ASCE, Vol. 116, No. 7, pp. 1813-1834, July, 1990.
- Kishi, N., W.-F. Chen, Y. Goto, and K. G. Matsuoka, "Design Aid of Semi-rigid Connections for Frame Analysis," *Engineering Journal*, AISC, Third Quarter, pp. 90-107, 1993.
- Krishnamurthy, N., and D. E. Graddy, "Correlation Between 2- and 3-Dimensional Finite Element Analysis of Steel Bolted End-Plate Connections," *Computers & Structures*, Vol. 6, pp. 381-389, 1976.
- Manual of SAP90 Structural Analysis Programs. Berkeley, California: Computers & Structures, Inc., 1988.



## LOW-CYCLE FATIGUE BEHAVIOUR AND DAMAGE ASSESSMENT OF SEMI-RIGID BEAM-TO-COLUMN CONNECTIONS IN STEEL

### **Carlo A. Castiglioni**

Associate Professor  
Structural Engineering Dept.  
Politecnico di Milano  
Italy

### **Luis Calado**

Associate Professor  
Instituto Superior Técnico  
Civil Engineering Dept.  
Portugal

Carlo A. Castiglioni, born 1956, received his laurea in Civil Engineering from Politecnico di Milano in 1980. He was part of the Visiting Faculty at Lehigh University, USA, in 1984. After being appointed Associate Professor at La Sapienza University in Rome in 1992, he is presently at Politecnico di Milano. His main research fields are high and low cycle fatigue of steel structures.

Luis Calado, born 1958, received his MSc in Structural Engineering in 1985 and his PhD in Civil Engineering in 1989 from Technical University of Lisbon. Presently he is Associate Professor at the Civil Engineering Department of the Technical University of Lisbon. His main research field is seismic behaviour and design of steel structures. He is also partner in a consulting company for structural design.

### **Summary**

A research was carried out in co-operation between Politecnico di Milano and Instituto Superior Técnico to investigate the behaviour of semi-rigid beam-to-column connections in steel under low-cycle fatigue and to try to establish possible classes of low-cycle fatigue resistance similar to those existing for structural details under high cycle fatigue. Different typologies of beam-to-column connections were experimentally and numerically studied, and a general failure criterion was proposed for steel components under low-cycle fatigue.

### **1. Introduction**

Following the Northridge Earthquake of January 17, 1994 several cases were reported of steel frame buildings which did not collapse, yet exhibited significant structural damage, with local failures of steel structural members or their connections. Such failures, however, did not result in severe overall deformations, thus remaining hidden behind undamaged architectural panels. A variety of local collapses was observed, among which the recurrent case was identified in the failure of welded beam-to-column joints in moment resisting space frames. Investigations [1] have been carried out about the nature and the causes of the observed failures and have shown that several topics pose unsolved problems, thus providing subjects of primary importance for research programs.

In design of steel structures it is in general assumed that the behaviour of connections is rigid or pinned, although their real behaviour is intermediate. Interest in this type of approach is recently decreased because was recognised that it does not allow a full comprehension of the real structural behaviour, and that leads to an economically non competitive design.



On the contrary, interest in semi-rigid connections is widely increased in the last 15 years, and several numerical and experimental research studies were performed all over the world. Most of these studies were carried out on the static behaviour of connections [2], and limited information are available on their cyclic response [3-7]. In addition to these and other experimental researches, a number of numerical models were also developed by various authors. Most of these models are empirical, and need experimental results for calibrating the various parameters assumed as governing the joint behaviour.

Since 1985 a co-operation between the Instituto Superior Técnico in Lisbon and the Politecnico of Milano was activated and several research programs in the field of the seismic behaviour of steel structures were performed.

This paper presents the results of a research on the low cycle fatigue behaviour of semi-rigid steel beam-to-column connections. Four different typologies of connections were realised and tested in a multi-specimen program in order to obtain information regarding the behaviour of different connections, and to verify the validity of the damage accumulation model and failure criterion presented in [8].

## **2. Experimental research**

### **2.1 Test set-up**

The experimental set-up was designed in order to simulate the conditions of different members or connections within the frame structure. It consists mainly in a foundation, a supporting girder, a reaction wall, a power jackscrew and a lateral frame. The power jackscrew, which displays a 1000 kN capacity and a 400 mm stroke, is attached by means of pretensioned bolts to the reaction element. Specimens are connected to the supporting girder. Lateral frames were designed to prevent specimens lateral displacement.

### **2.2 Test specimens**

The specimens consisted of a beam attached to a column by means of four different details, which represent frequent solutions adopted in steel construction: bolted web and flanges cleats (BCC1), extended end plate (BCC2), flange plates (welded to the column and bolted to the beam) with web cleats (BCC3), and beam flanges welded to the column with bolted web cleats (BCC4). For each typology several specimens were realised and tested, according to a multi-specimen testing program.

The profile used for columns and beams in all specimens was a HEA120 in Fe360. For the web and flanges cleats specimens 100x100x10 angles in Fe360 were adopted. Bolts used in all specimens were M16, grade 8.8; in the case of flange plates with web cleats specimens and of extended end plate connections, bolts were preloaded according to EC3 provisions. All welds were full penetration butt welds.

Specimens were fabricated in order to simulate field conditions, following the procedures of workmanship and quality control as required by applicable standards. This applies particularly to welding and bolting. Specimens were instrumented with LVDTs, measuring namely, the

vertical displacement of the joint and the relative and absolute rotation of the cross-section and joint.

### 2.3 Loading histories

The choice of a testing history associated to a testing program depends on the purpose of the experiment, type of test specimen and type of anticipated failure mode. However, as it is also clearly stated in ATC Guidelines [9], a multi-specimen testing program is needed if a cumulative damage model is to be developed for the purpose of assessing the performance of a component under arbitrary loading histories. In particular a cumulative damage model may be adopted to evaluate the cumulative effect of inelastic cycles on a limit state of acceptable behaviour. The deformation amplitudes for the tests should be selected so that they cover the range of interest for performance assessment. The total amplitude of the cyclic rotation  $\Delta\phi$  adopted in this research ranges between 5.00 and 12.00  $\phi_y$  where  $\phi_y$  is the yield rotation of the connection. All specimens were initially subjected to four cycles in the elastic range with total amplitude of 0.50  $\phi_y$ , 1.00  $\phi_y$ , 1.50  $\phi_y$  and 2.00  $\phi_y$ .

## 3. Experimental results

Test results as hysteresis loops in a moment-rotation diagram ( $M-\phi$ ) and respective failure mode for each typology of beam-to-column connection are presented in Figures 1 - 4, together with some comments on the behaviour of each type of connections.

### 3.1 Bolted web and flanges cleats connections (BCC1)

These connections are characterised by large slippage, that seems to increase, with the number of cycles, although the displacement amplitude is constant.

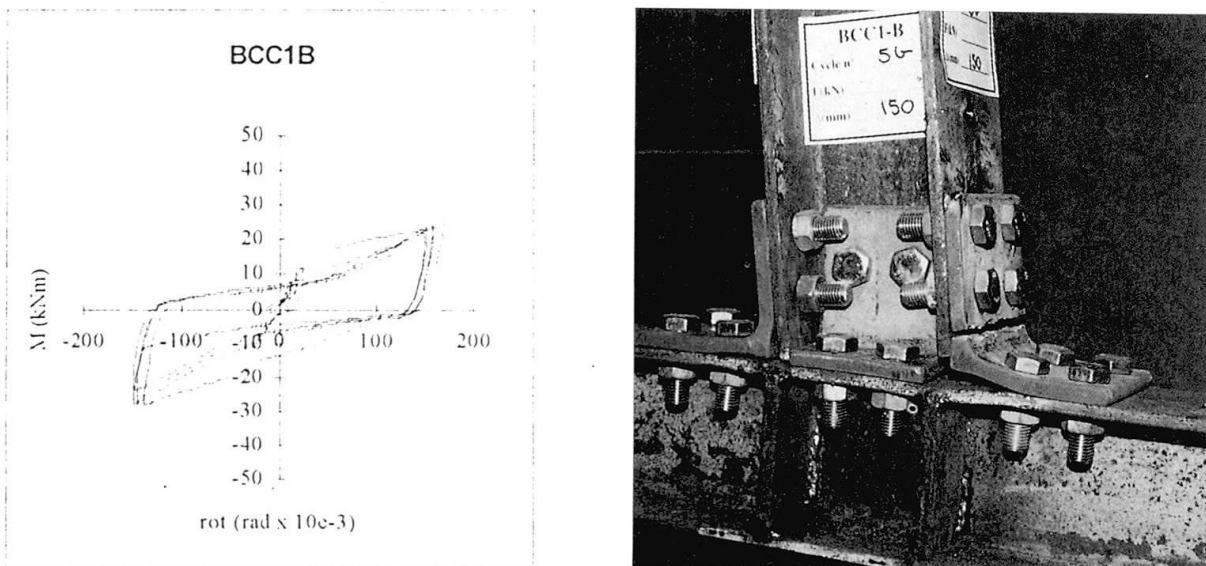


Fig. 1. Experimental moment-rotation diagram and failure mode of BCC1 connection type.



Increment of plastic deformations in the angles produced progressive deterioration of absorbed energy (Fig. 5). Slip occurred mainly between the beam flange and the angle leg due to ovalization of the holes. For all specimens collapse was caused by cracking in the angles under tensile loading which propagated, with increasing the number of cycles, until complete failure.

### 3.2 Extended end plate connections (BCC2)

These connections are characterised by regular hysteresis loops without any slippage and with regular deterioration of the absorbed energy (Fig. 5) and the maximum moment at the end of each cycle (Fig. 2). For all specimens, a plastic hinge developed in the beam approximately at a distance equal to the height of the profile. Local buckling produces deterioration of absorbed energy and maximum moment capacity. Large deformations at plastic hinge induce cracking in the beam flange leading, in a few cycles, to complete failure of the cross-section.

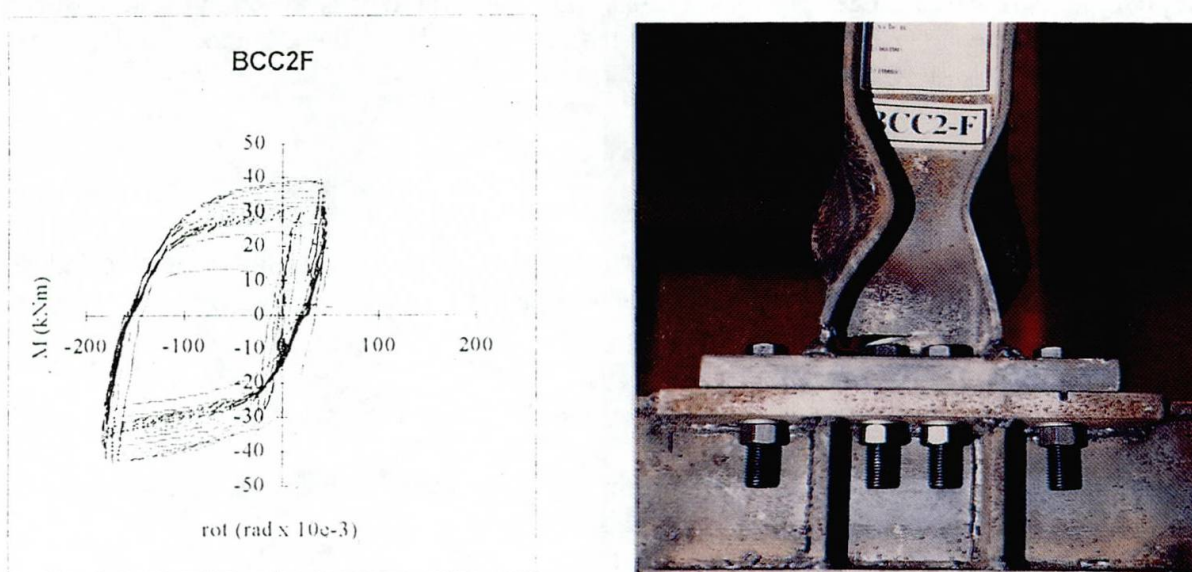


Fig. 2. Experimental moment-rotation diagram and failure mode of BCC2 connection type.

### 3.2 Bolted flange plates (welded to the column) with web cleats (BCC3)

This type of connection exhibited slippage between flange plates and beam flange due to ovalization of the holes, but this phenomenon has lower importance when compared with web and flanges cleats connections. During the test, a progressive deterioration of the absorbed energy (Fig. 6) took place. The flange plate had a similar behaviour as the angles in BCC1 type under bending deformation but no evident separation between beam and column was observed. Failure was due to cracking at welding connecting the flange plates to the column flange. These cracks propagated with increasing the number of cycles until complete failure.

### 3.4 Welded flanges with bolted web cleats connections (BCC4)

These connections are characterised by high elasticity and great regularity in the shape of the loops with gradual deterioration of the absorbed energy (Fig. 6). Large plastic deformations developed in the panel zone of the column. In most cases failure was due to cracking at toe of welding connecting the beam flanges to the column one. These cracks propagated with

increasing the number of cycles until complete failure. Propagation was observed either in the beam flange or in the column one, where due to the presence of other weldings connecting transversal stiffeners to the column web and flanges, complete separation of the column flange in the panel zone was observed (Fig. 4). Large ovalization was always observed due to high bearing stresses in the bolts of the web cleats.

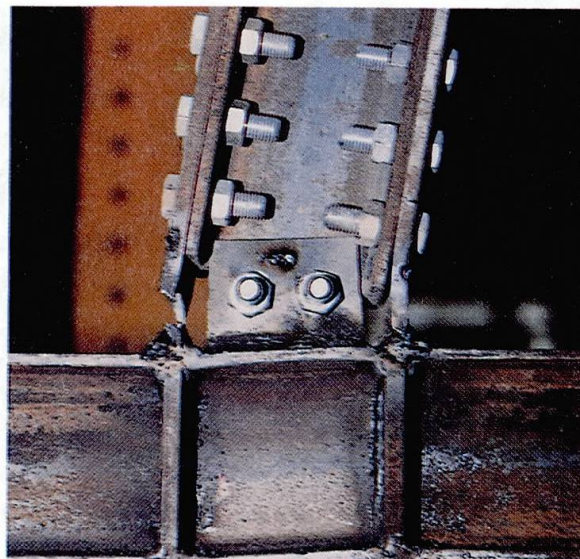
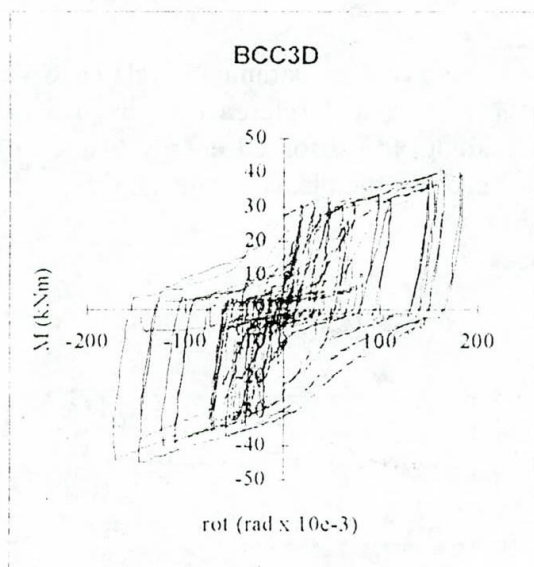


Fig. 3. Experimental moment-rotation diagram and failure mode of BCC3 connection type.

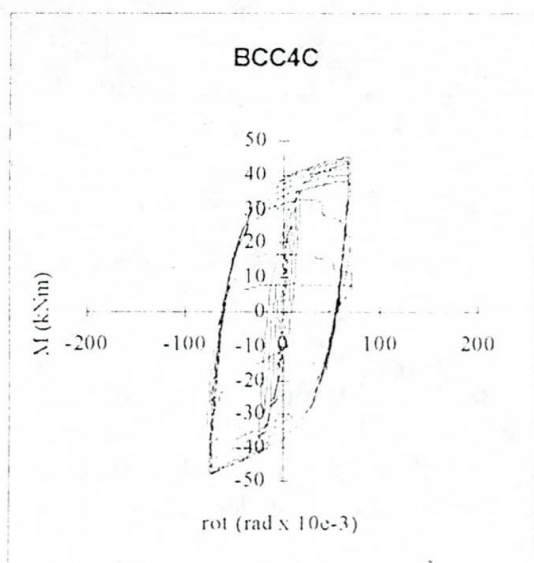


Fig. 4. Experimental moment-rotation diagram and failure mode of BCC4 connection type.

#### 4. Failure criterion

As previously stated, aim of the research was also the development of a failure criterion, to be adopted together with a damage model for the assessment of low cycle fatigue resistance. It is particularly interesting to formulate some failure criterion based on the achievement of a given



level of deterioration of the mechanical properties of the material. In fact, by means of such a collapse criterion, the limit state at which a structural component is considered out-of-service, can be a-priori defined. Such a situation, of course, may not coincide with actual collapse of the component. However, in order to be applied in standard design procedures, such a collapse criterion must allow an assessment of the failure conditions as close to reality as possible, and always on the safe side.

Previous experience indicated that such a criterion might be based on parameters related with the energy absorption capacity of the component. For this reason, with reference to the present research program, that considered constant amplitude loading, the absorbed energy  $E$  in each cycle has been related to the one  $E_0$  absorbed in the first cycle in the plastic range, as shown in Figs. 5 and 6.

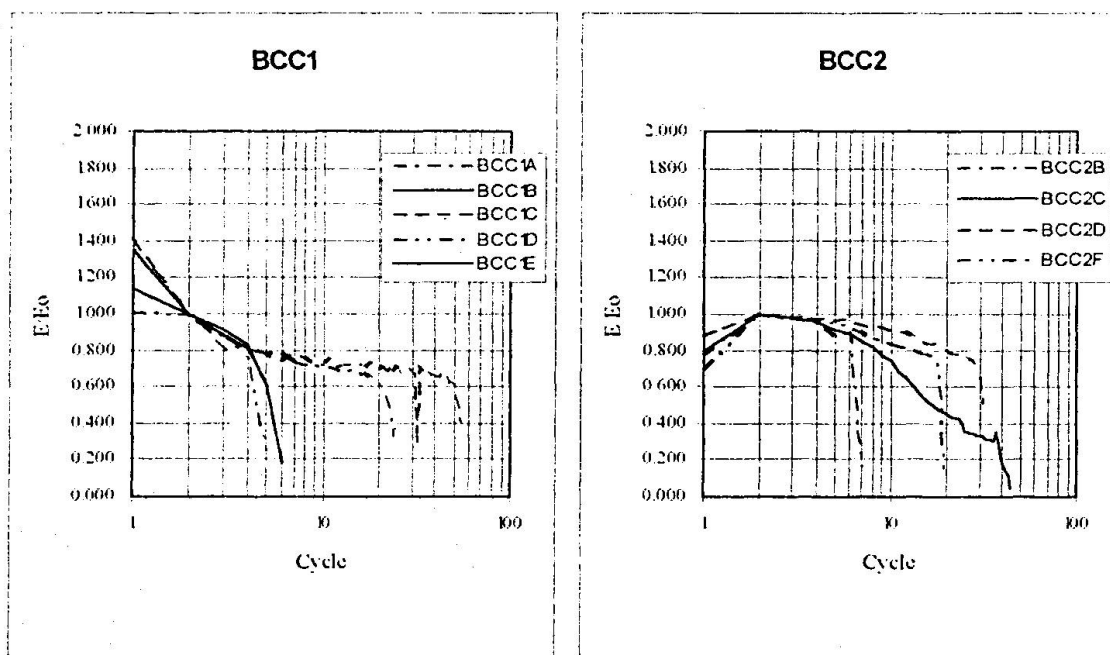


Fig. 5.  $E/E_0$  versus number of the cycle for BCC1 and BCC2 connection types.

It can be noticed that after a stage of nearly constant reduction of the ratio  $E/E_0$ , collapse is reached in a few cycles (representing nearly 5% of the total number of cycles to failure), in which an abrupt reduction of the energy absorption capacity takes place. It can also be noticed that this abrupt reduction occurs when the ratio  $E/E_0$  reaches a value which seems to be a constant, independently on the typology of the connection.

Based on this experimental evidence the following failure criterion can be formulated having a general validity for structural steel components:

$$\frac{E}{E_0} \leq \alpha \quad (1)$$

In this equation  $\alpha$  is a parameter whose value represents a limit to the reduction of energy absorption capacity beyond which it might be assumed that failure occurs, and should be

determined by fitting the experimental results. The current research program showed that values for  $\alpha$  ranging between 0.50 and 0.70 can be adopted. It should however be noticed that, in general, the difference between the number of cycles corresponding to the extreme values of the suggested range is a very small percentage of the total number of cycles, and that a value of  $\alpha$  equal to 0.50 might be assumed.

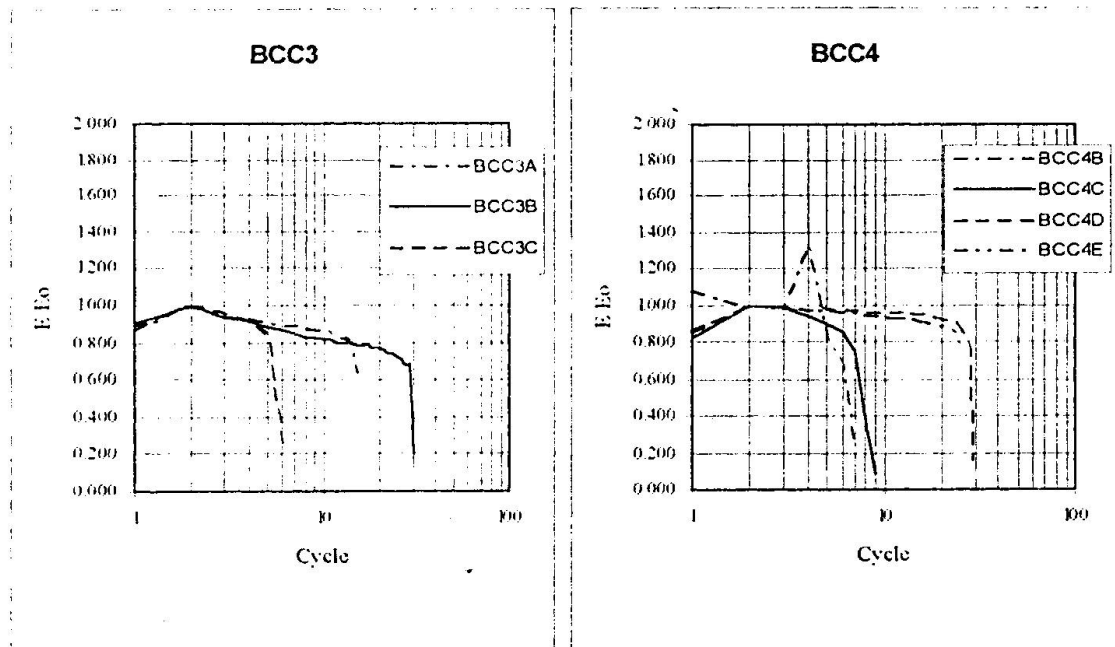


Fig. 6.  $E/E_0$  versus number of the cycle for BCC3 and BCC4 connection types

This value is not to be considered as the best fit of experimental results, but can be regarded as possible reference value in damage assessment procedures. Of course, to be adopted for design purposes, an appropriate safety factor should be assumed, based on safety and reliability considerations.

## 5. Cumulative damage model

From these tests results as well as those carried out by other authors [10,11] it was noticed that, in good agreement with other previous studies [12,13], for all structural components (beams, beam columns, welded joints, beam-to-column connections), the relationships which best fitted the experimental results in terms of cycle amplitude and number of cycles to failure  $N_f$ , were exponential functions of the type:

$$N_f = a \left( \frac{\Delta s}{s_y} \right)^b \quad (2)$$

where  $a$  and  $b$  are constant parameters to be calibrated on experimental results,  $\Delta s$  is the cycle amplitude in terms of generalised displacement component, and  $s_y$  is the yield value of  $s$ .



the design and damage assessment procedures for steel structures under low and/or high cycle fatigue.

In practice, by adopting the S-N curves of EC3 [16], and adopting Miner's rule [17], the proposed damage model becomes:

$$D = \frac{1}{K} \sum_1^L n_i \left( \frac{\Delta s_i}{s_y} \sigma(F_y) \right)^3 \quad (3)$$

where  $K$  is a constant value tabulated by EC3, depending on the fatigue strength category of the detail,  $n_i$  is the number of occurrences of cycles having an amplitude  $\Delta s_i$ , the summation is extended to the number  $L$  of different cycle amplitudes  $\Delta s_i$  to be considered, and  $\sigma(F_y)$  is the stress corresponding to first yield [15].

An equivalent stress range of constant amplitude, that equals the variable amplitude damage for the total number of applied stress cycles, can also be derived:

$$\Delta \sigma_{eq}^* = \left[ \sum_1^L \frac{n_i}{N_f} \left( \frac{\Delta s_i}{s_y} \sigma(F_y) \right)^3 \right]^{\frac{1}{3}} \quad (4)$$

This value should be used when plotting, on S-N diagrams, data from variable amplitude tests.

## 6. Re-elaboration of test results

Figure 7 shows the test data for beam-to-column connections tested under constant amplitude loading (BCCi-Lisbon) together with tests results performed with variable loading amplitude on double angle connections (U.C.-Berkley) [4], top-and-seat angle connections (S.U.N.Y.-Buffalo) [18], top-and-seat angle connections (VPH V.A.-Lisbon) [19] and beam-to-column connections (BCCi-V.A.-Lisbon) [20].

Beam-to-column connections of the same typology, belong to the same fatigue strength category, despite the adopted profiles are different. Furthermore, the fatigue strength of the connection can be directly related to its ductility. For example, bolted web and flange cleats are less ductile than the connection with welded flanges and bolted web cleats. This results, in lower fatigue strength for BCC1 connections and higher for BCC4. BCC2 and BCC3 connections show a similar behaviour, intermediate between the previous ones.

Independently on the category of fatigue resistance pertinent to each typology of the connection, it is important to notice that the slope of the line fitting (in a log-log plot) the low cycle fatigue test data, is nearly -3. This is in good agreement with the results of research on high cycle fatigue.

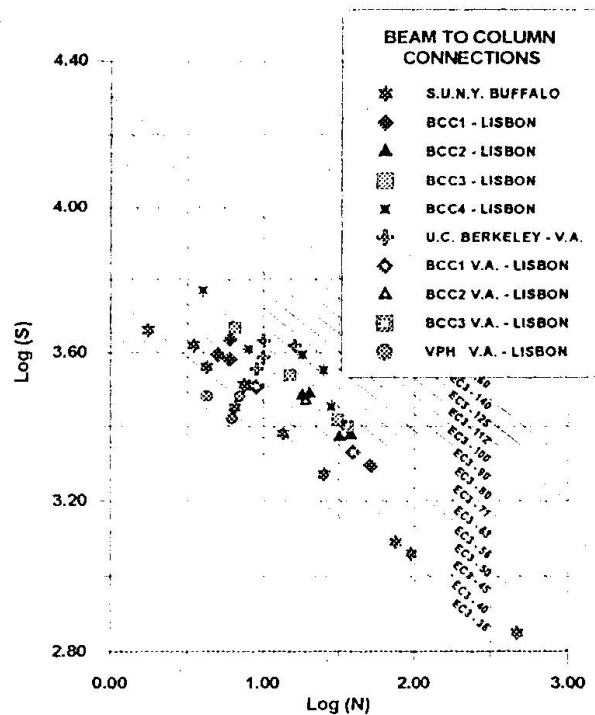


Fig. 7. Fatigue strength of beam-to-column connections.

## 7. Concluding remarks

This paper presents an approach to the study of the seismic behaviour of beam-to-column connections which is based on methodologies commonly adopted for fatigue damage assessment. In particular, it is tried to extrapolate the procedures usually adopted for high cycle fatigue to the low cycle fatigue range, which is the behaviour to be expect in structural steel members and connections under seismic actions.

In order to be adopted in current design practice, the proposed model requires the definition of the fatigue strength category of various typologies of the connections, i. e., of the appropriate S-N curve to be associated with each type of detail. This can be done either by means extensive experimental research or by numerical modeling. Such models should, however, be calibrated on tests results. In any case a reliable failure criterion must be defined, allowing conservative definition of the number of cycles to failure, i. e. of the conditions corresponding to specimen collapse. A possible failure criterion having a general validity and giving consisting results for a number of structural components has been proposed in this paper.

## 8. Acknowledgements

The financial support from JNICT, from M.U.R.S.T. 40% and from E.C. "Human Capital and Mobility" "Seismic Protection of the Built Heritage" is gratefully acknowledged.



## 9. References

- [1] SAC Joint Venture, (1995), Interim Guidelines: Evaluation, Repair, Modification and Design of Steel Moment Frames, Report N° SAC-95-02, *Federal Emergency Management Agency, FEMA 267*.
- [2] Nethercot, D. and Zandonini, R., (1989), Methods of prediction of joint behaviour, *Structural Connections: Stability and Strength*. Ed. R. Narayanan, Elsevier Applied Publishers.
- [3] Ballio, G., Calado, L., De Martino, A., Faella, C. and Mazzolani, F., (1987), Indagine sperimentale sul comportamento ciclico di nodi trave-colonna in acciaio, *Costruzioni Metalliche*, N° 2.
- [4] Astaneh, A. Nader, M. N. and Malik, L. (1989), Cyclic behaviour of double angle connections, *ASCE, Journal of Structural Engineering*, vol. 115, n.5.
- [5] Bernuzzi, C., R. Zandonini and P. Zanon, (1992), Semi-Rigid Steel Connections Under Cyclic Loads, *First World Conference on Constructional Steel Design*, Acapulco.
- [6] Popov, E. (1985), Flexibility of steel seismic moment connections. *Connection flexibility and steel frames*, Edited by Wai-Fah Chen.
- [7] Korol, R., A. Ghobarah and A. Osman (1990). Extended end-plate connections under cyclic loading: behaviour and design. *Journal of Constructional Steel Research*, vol. 16.
- [8] Ballio, G., Calado, L. and Castiglioni, C.A., (1996), Low Cycle Fatigue and Fracture of Structural Steel Members and Connections, *Fatigue & Fracture of Engineering Materials & Structures*. (To be published)
- [9] ATC - Applied Technology Council (1992), Guidelines for cyclic seismic testing of components of steel structures, *ATC 24*.
- [10] Ballio, G. and Castiglioni, C.A. (1994), Seismic behavior of steel sections, *Journal of Constructional Steel Research*, n.29, pp 21-54
- [11] Ballio G. and Chen Y. (1993), An experimental research on beam to column joints: exterior connections, *Proc. C.T.A., Viareggio*, pp. 110-120.
- [12] Coffin, L. F. (1954), A study of the effects of cyclic thermal stresses on a ductile method, trans. *ASME*, 76.
- [13] Mason, S. (1954), Behaviour of material under conditions of thermal stress, *Heat Transfer Symposium, NACA TN 2933*.
- [14] Wöhler A. (1860), *Zeitschrift für Bauwesen*, vol.10.
- [15] Ballio, G., Castiglioni, C.A. (1995), A unified approach for the design of steel structures under low and/or high cycle fatigue, *Journal of Constructional Steel Research*, n.34, pp75-101
- [16] CEN (1992), Eurocode 3: Design of Steel Structures-Part 1-1: General rules and rules for buildings, *EN1993-1-1*, February.
- [17] Miner, M.A. (1945), Cumulative damage in fatigue, *Journal of Applied Mechanics*, Sept.
- [18] Mander, J.B., Chen, S.S. and Pekcan, G. (1994), Low-cycle fatigue behavior of semi-rigid top-and-seat angle connections, *Engineering Journal, American Institute of Steel Construction*, 3rd quarter, pp 111-122
- [19] Calado L. and Ferreira J. (1994), Cyclic behaviour of steel beam to column connections: an experimental research, *Proc. Int. Workshop on Behaviour of Steel Str. in Seismic Areas*, Timisoara, E and FN SPON, pp. 381-389.
- [20] Calado, L and Castiglioni, C., (1995), Low-cycle fatigue testing of semi-rigid beam-to-column connections. *3rd International Workshop on Connections in Steel Structures*, Trento.